Nicotinamide Phosphoribosyltransferase Inhibitors, Design, Preparation, and Structure-Activity Relationship

ARTICLE *in* JOURNAL OF MEDICINAL CHEMISTRY · OCTOBER 2013

Impact Factor: 5.45 · DOI: 10.1021/jm4009949 · Source: PubMed

Journal of Medicinal Chemistry

Article

pubs.acs.org/jmc

Nicotinamide Phosphoribosyltransferase Inhibitors, Design, Preparation, and Structure−Activity Relationship

Mette K. Christensen,[†,▽] Kamille D. Erichsen,[†,▲] Uffe H. Olesen,[†,§] Jette Tjørnelund,[†] Peter Fristrup,[⊥] Annemette Thougaard,[†,○] Søren Jensby Nielsen,[†,◆] Maxwell Sehested,[†,§] Peter B. Jensen,[†,¶] Einars Loza,[#] Ivars Kalvinsh,[#] Antje Garten,[∥] Wieland Kiess,[∥] and Fredrik Björkling*[,†,‡]

[†]Topotarget A/S, Symbion, Fruebjergvej 3, Copenhagen DK-2100, Denmark

[‡]Department of Drug Design and Pharmacology, Faculty of Health and Medical Sciences, University of Copenhagen, Universitetsparken 2, Copenhagen DK-2100, Denmark

[§]Experimental Pathology Unit, National University Hospital, Biocentre, Ole Maaloes Vej 5, Copenhagen DK-2200, Denmark

[∥]Center for Pediatric Research, Hospital for Children and Adolescents, University of Leipzig, Liebigstr. 21, Leipzig 04301, Germany

[⊥]Department of Chemistry, Technical University of Denmark, Kemitorvet 207, Lyngby DK-2800, Denmark

[#]Latvian Institute of Organic Synthesis, Aizkraukles 21, Riga LV-1006, Latvia

Supporting Information

ABSTRACT: Existing pharmacological inhibitors for nicotinamide phosphoribosyltransferase (NAMPT) are promising therapeutics for treating cancer. By using medicinal and computational chemistry methods, the structure−activity relationship for novel classes of NAMPT inhibitors is described, and the compounds are optimized. Compounds are designed inspired by the NAMPT inhibitor APO866 and cyanoguanidine inhibitor scaffolds. In comparison with recently published derivatives, the new analogues exhibit an equally potent antiproliferative activity in vitro and comparable activity in vivo. The best performing compounds from these series showed subnanomolar antiproliferative activity toward a series of cancer cell lines (compound **15**: IC_{50} 0.025 and 0.33 nM, in A2780 (ovarian carcinoma) and MCF-7 (breast), respectively) and potent antitumor in vivo activity in well-tolerated doses in a xenograft model. In an A2780 xenograft mouse model with large tumors (500 mm^3), compound **15** reduced the tumor volume to one-fifth of the starting volume at a dose of 3 mg/kg administered ip, bid, days 1−9. Thus, compounds found in this study compared favorably with compounds already in the clinic and warrant further investigation as promising lead molecules for the inhibition of NAMPT.

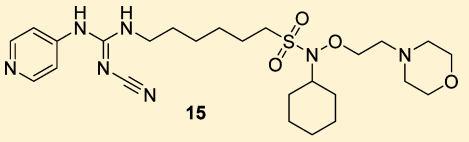

15

Biological Data: IC_{50}
0.025 nM in A2780
0.33 nM in MCF-7

INTRODUCTION

Inhibition of nicotinamide adenine dinucleotide (NAD) production has recently been suggested as a principle for inducing death of cells with high demand for this dinucleotide.[1] This is particularly true for cancer cells due to increased metabolism and high activity of NAD-consuming enzymes. NAD is an essential cofactor in redox reactions and as such is involved in cellular energy production and metabolism without being substantially consumed. However, besides being a cofactor, NAD serves as the substrate for mono-ADP-ribosyltransferases,[2] poly-ADP-ribose polymerases (PARPs),[3] and sirtuins,[4] all of these converting NAD to nicotinamide. Also, NAD is consumed as the precursor for a number of Ca^{2+}-releasing second messengers (e.g., cADPR and NAADP).[5,6]

Thus, the increased dependence on glycolysis and elevated expression or activity of PARPs[7−9] and sirtuins,[4] characteristic for malignant cells, make these more sensitive to NAD availability as compared with normal cells.[10,11]

In the organism, several pathways for the synthesis of NAD are known. Besides the de novo pathway using tryptophan as a precursor, NAD can alternatively be synthesized or resynthesized from nicotinamide, a sequence where nicotinamide phosphoribosyltransferase (NAMPT) catalyzes the rate-limiting step.[12−14] Thus, inhibition of NAMPT enzyme activity causes a direct inhibition of NAD production. Importantly, normal cells can use an alternative pathway for NAD synthesis from nicotinic acid (NA), catalyzed by nicotinic acid phosphoribosyltransferase (NAPRT).[15−17] Unlike most normal tissues, many cancer cell lines, and primary tumors, are deficient in NAPRT activity.[18] Furthermore, an increased concentration of NAMPT in colorectal, ovarian, and prostate cancer cells has been reported.[10,19,20] Altogether, inhibition of NAD production via NAMPT inhibition is suggested to be a valid principle for selective inhibition of cancer cell growth and as such represents an attractive target for drug discovery.

A few classes of NAMPT inhibitors have been reported such as compounds APO866 (**1**)[21] and CHS828 (**2**),[22] which have entered the clinic, and more recent structures such as TRON-8[23] and CB30865[24] for which biological data have been

Received: July 2, 2013

   dx.doi.org/10.1021/jm4009949 | J. Med. Chem. XXXX, XXX, XXX−XXX

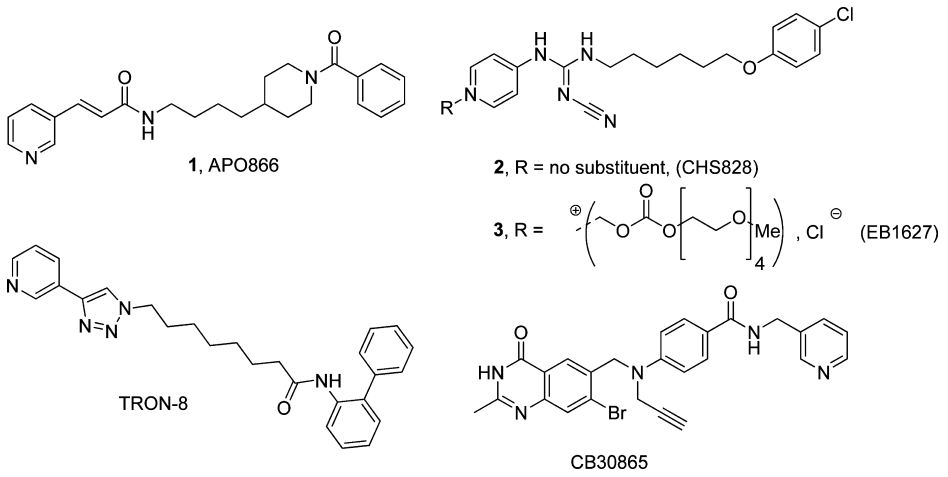

Figure 1. NAMPT inhibitors. **1**, APO866 (for activity, see Table 1); **2**, CHS-828 (for activity, see Table 1); **3**, EB 1627 (prodrug of CHS828); TRON-8 (IC_{50} (SH-SY5Y) 3.8 nM);[23] and CB30865 (IC_{50} (W1L2) 2.8 nM).[37]

Scheme 1. Convergent Synthesis of 2-Cyanoguanidine Derivatives 11−25

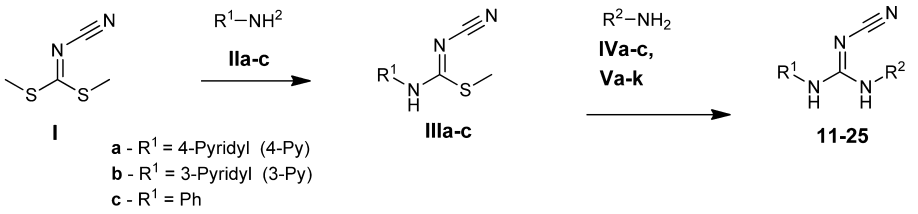

No	R^1	R^2
IVc, 11	4-Py	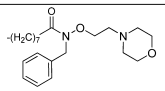
IVa, 12	4-Py	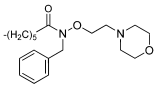
IVb, 13	Ph	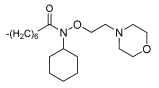
Vk, 14	4-Py	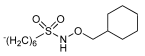
Ve, 15	4-Py	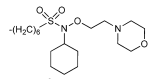
IVb, 16	3-Py	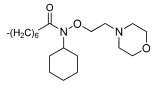
Vi, 17	4-Py	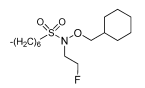
Vg, 18	4-Py	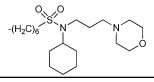

No	R^1	R^2
Vj, 19	4-Py	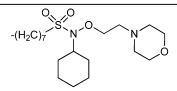
Va, 20	4-Py	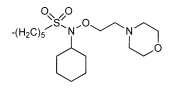
Vd, 21	4-Py	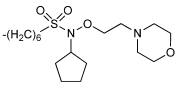
Vc, 22	4-Py	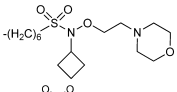
Vf, 23	4-Py	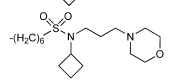
Vb, 24	4-Py	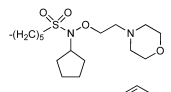
Vh, 25	4-Py	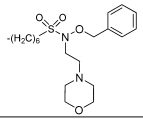

reported (Figure 1). Biological data for NAMPT inhibitor MCP-8640 is also reported, but no chemical structure is reported.[25] These NAMPT inhibitors show potent antiproliferative activity in a spectrum of cancer cell lines and in vivo efficacy in both solid tumors and leukemia in preclinical studies.[26,27] A comprehensive literature review on NAMPT inhibitors including patents was recently published.[28] Originally, **1** was developed as an inhibitor of NAMPT and displays antiproliferative activities comparable to compound **2** for which the molecular target was unknown until recently.[29−31] Safety, pharmacokinetics, and biological effect of compounds **1** and **2** (and a prodrug thereof, **3**, Figure 1) have been reported from five phase I clinical trials performed in patients with advanced disease.[32−34] In these trials, not surprisingly in phase I, no objective response was found, and for both compounds, the dose-limiting toxicity was found to be thrombocytopenia.

dx.doi.org/10.1021/jm4009949 | J. Med. Chem. XXXX, XXX, XXX−XXX

Scheme 2. Synthesis of 2-Cyanoguanidine Derivatives 4−10 via Carboxylic Acid Intermediates VIIa−e

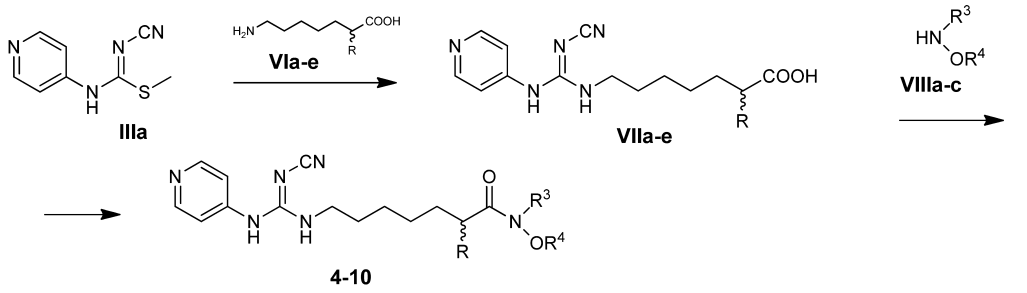

No	R
VIa, VIIa	H
VIb, VIIb	(R)-Me
VIc, VIIc	(S)-Me
VId, VIId	(R)-Bn
VIe, VIIe	(S)-Bn

No	R^3	R^4
VIIIa	H	
VIIIb	Bn	
VIIIc		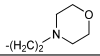

No	R	R^3	R^4
4	H	H	
5	H	Bn	
6	(S)-Me	H	
7	(R)-Me	H	
8	(S)-Bn	H	
9	(R)-Bn	H	
10	H		

Scheme 3. Convergent Synthesis of 1,2-Diaminocyclobutene-3,4-dione Derivatives 26−36

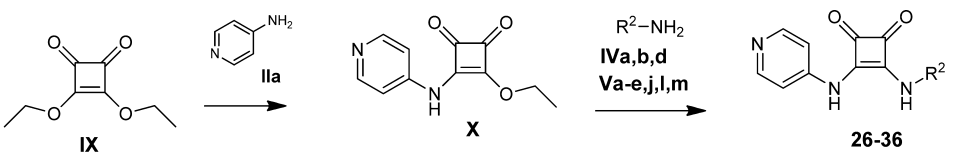

No	R^2
IVb, 26	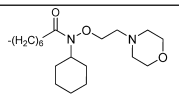
Vl, 27	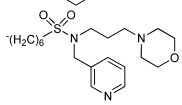
IVd, 28	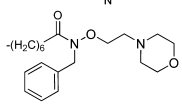
IVa, 29	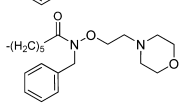
Vm, 30	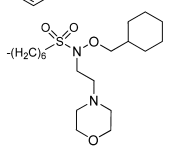
Ve, 31	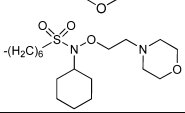

No	R^2
Vj, 32	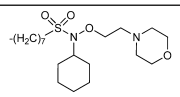
Va, 33	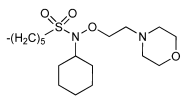
Vd, 34	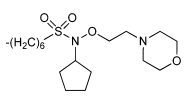
Vc, 35	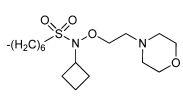
Vb, 36	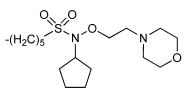

Compound **2** was tested in an oral formulation but was later transformed to a prodrug, compound **3**, to obtain improved pharmacokinetics.[35,36] To obtain good exposure, both compounds **1** and **3** were administered iv using long-term continued infusion.[33,34] Both compounds have entered phase II clinical trials; however, results from these trials are not yet available.

dx.doi.org/10.1021/jm4009949 | J. Med. Chem. XXXX, XXX, XXX−XXX

Scheme 4. Synthesis of *N,N′*-Disubstituted Urea Derivatives 37, 38, and 40−50

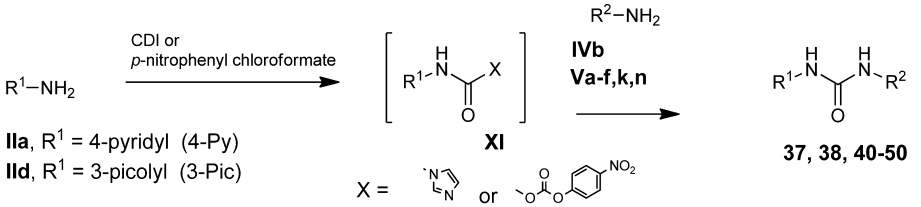

No	R^1	R^2
Ve, 37	4-Py	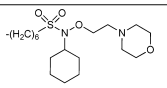
IVb, 38	3-Pic	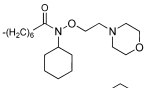
Vm, 40	4-Py	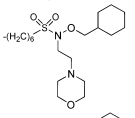
Vm, 41	3-Pic	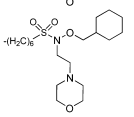
Va, 42	4-Py	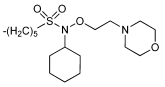
Vj, 43	4-Py	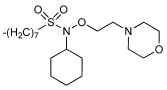
Va, 44	3-Pic	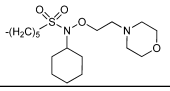

No	R^1	R^2
Vj, 45	3-Pic	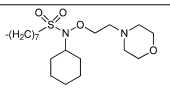
Vd, 46	3-Pic	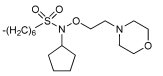
Vc, 47	3-Pic	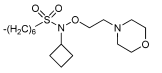
Vf, 48	3-Pic	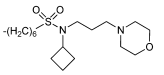
Vn, 49	3-Pic	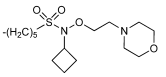
Vb, 50	3-Pic	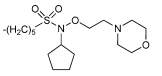

Scheme 5. Synthesis of *N,N′*-Disubstituted Thiourea Derivatives 39 and 51

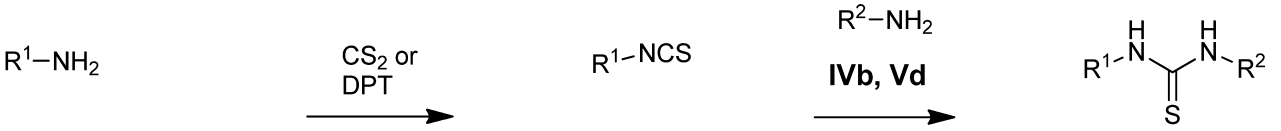

No	R^1	R^2
IVb, 39	3-Pic	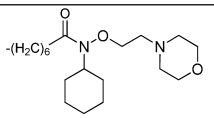
Vd, 51	4-Py	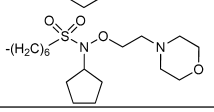

Inspired by these results and with the aim of finding compounds with improved toxicological and activity properties, we here report the structure−activity relationship (SAR) for a new series of NAMPT inhibitors based on structural modifications of compounds **1** and **2**. The results from the SAR study were rationalized, and new compounds were designed using computational chemistry methods.

RESULTS AND DISCUSSION

Chemistry. A series of 2-cyanoguanidines **11**−**25** was synthesized using a general strategy (Scheme 1). Treatment of dimethyl cyanocarbonimidodithioate (**I**) with 4-pyridylamine (**IIa**), 3-pyridylamine (**IIb**), or aniline (**IIc**) produced methyl *N′*-cyano-*N*-arylcarbamimidothioates **IIIa**−**c**, which were condensed with preassembled hydroxamate amines **IVa**−**c** or

dx.doi.org/10.1021/jm4009949 | J. Med. Chem. XXXX, XXX, XXX−XXX

Scheme 6. Preparation of Hydroxylamines VIIIa,b,d,e

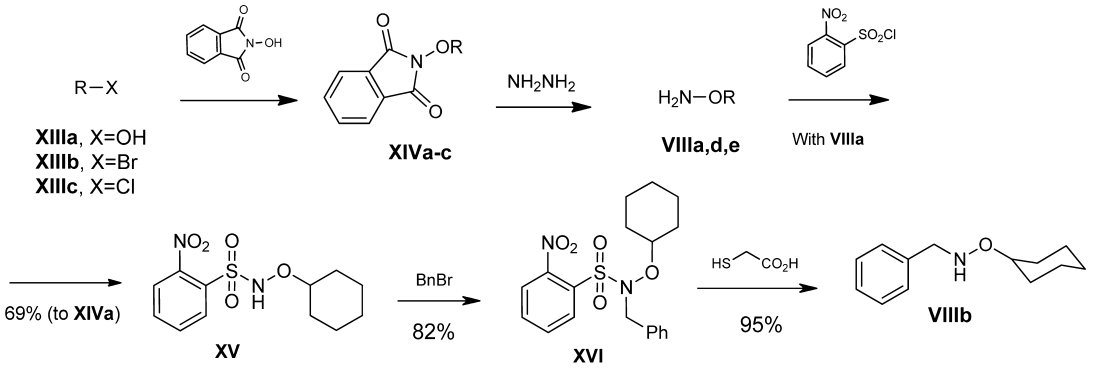

No	R
XIIIa, XIVa, VIIIa	Cyclohexyl
XIIIb, XIVb, VIIId	cyclohexylmethyl
XIIIc, XIVc, VIIIe	2-(4-morpholinyl)ethyl

Scheme 7. Preparation of Hydroxylamines VIIIc,f,h and Amines VIIIg,i

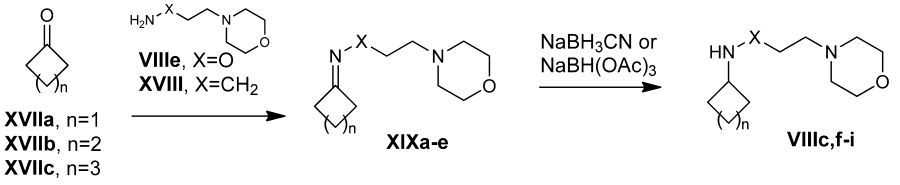

No	n	X
XIXa, VIIIf	**1**	**O**
XIXb, VIIIg	1	CH_2
XIXc, VIIIh	2	O
XIXd, VIIIc	3	O
XIXe, VIIIi	3	CH_2

sulfonamide amines **Va−k** to give the corresponding 2-cyanoguanidines **11−25**.

Although this convergent approach was successful in most cases, a stepwise formation of the side chain was used for some 2-cyanoguanidine derivatives such as **4−10** (Scheme 2).

Thus, the condensation of methyl *N*′-cyano-*N*-(pyridin-4-yl)carbamimidothioate (**IIIa**) with 7-aminoheptanoic acid (**VIa**) or optically active 2-methyl or 2-benzyl-7-amino-heptanoic acids **VIb−e**[38] produced 7-guanidinoheptanoic acid derivatives **VIIa−e**. These intermediate acids **VIIa−e** afforded the target *N*-hydroxycarboxamides **4−10** when treated with hydroxylamines **VIIIa−c** in the presence of 1-ethyl-3-(3-dimethylaminopropyl)carbodiimide (EDC) or *O*-(7-azabenzo-triazol-1-yl)-*N*,*N*,*N*′,*N*′-tetramethyluronium hexafluorophos-phate (HATU).

A similar convergent approach to Scheme 1 was used for the preparation of a series of 1,2-diaminocyclobutene-3,4-diones **26−36** (Scheme 3).[39] Reaction of 3,4-diethoxy-3-cyclobutene-1,2-dione (**IX**) with 4-pyridylamine (**IIa**) afforded intermediate amidoester **X**, which was treated with amines **IVa**,**b**,**d** and **Va−e**,**j**,**l**,**m** to obtain target 1,2-diaminocyclobutene-3,4-diones **26−36**.

N,*N*′-Disubstituted urea derivatives **37**, **38**, and **40−50** were prepared by reacting of such carbonic acid derivatives as *N*,*N*′-carbonyldiimidazole (CDI) or 4-nitrophenyl chloroformate with 4-pyridylamine (**IIa**) or 3-picolylamine (**IId**) followed by appropriate preassembled amines **IVb** and **Va−f**,**k**,**n** (Scheme 4).

The *N*,*N*′-disubstituted thiourea derivative **39** was synthesized by the condensation of 3-picolylamine **IId** with di(2-pyridyl) thionocarbonate (DPT) followed by treatment of in situ formed intermediate isothiocyanate **XIIb** with amine **IVb**. The *N*,*N*′-disubstituted thiourea derivative **51** was prepared from amine **Vd** and isothiocyanate **XIIa**, which in turn was obtained from 4-pyridilamine **IIa** and carbon disulfide (Scheme 5).

The hydroxylamine intermediates **VIIIa**,**b**,**d**,**e** of carboxamide amines **IV** and sulfonamide amines **V** were synthesized starting from 2-hydroxyisoindoline-1,3-dione that was alkylated with cyclohexyl alcohol **XIIIa** upon Mitsunobu conditions, with cyclohexylmethyl bromide **XIIIb** in the presence of K_2CO_3 in DMSO or with 2-(4-morpholinyl)ethyl chloride (**XIIIc**) in the presence of 1,8-diazabicyclo[5.4.0]undec-7-ene (DBU) to give the O-substituted derivatives **XIVa−c**. Removal of the phthalimide protective group of compounds **XIVa−c** gave *O*-hydroxylamine derivatives **VIIIa**, **VIIId**, and **VIIIe**, respectively. Compound **VIIIa** was further converted into *N*-monobenzyl derivative **VIIIb** via 2-nitrobenzosulfonamide intermediates **XV** and **XVI** (Scheme 6).

Another series of N,O-disubstituted hydroxylamines **VIIIc**,**f−i** were prepared from cyclic ketones **XVIIa−c** and *O*-(2-morpholinoethyl)hydroxylamine (**VIIIe**) or 3-morpholinopro-

dx.doi.org/10.1021/jm4009949 | J. Med. Chem. XXXX, XXX, XXX−XXX

pan-1-amine (**XVIII**) by reductive amination (Scheme 7). Condensation of the ketones **XVIIa−c** with the amino compounds **VIIIe** or **XVIII** gave the corresponding intermediate oximes or imines **XIXa−e**, which were reduced to saturated structures **VIIIc,f−i**.

By a similar one-pot reductive amination protocol, *O*-(2-morpholinoethyl)hydroxylamine (**VIIIe**) and benzaldehyde afforded *N*-benzyl-*O*-(2-morpholinoethyl)hydroxylamine (**VIIIj**) (Scheme 8).

Scheme 8. Synthesis of *N*-Benzyl-*O*-(2-morpholinoethyl)hydroxylamine (VIIIj)

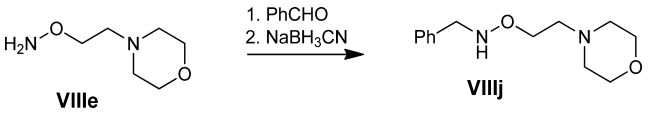

The hydroxamate amines **IVa−d** were prepared from *N*-Boc protected *ω*-amino hexanoic, heptanoic, and octanoic acids **XXa−c** that were condensed with hydroxylamine **VIIIj** in the presence of EDC or with hydroxylamine **VIIIc** in the presence of HATU to afford the corresponding hydroxamates **XXIa−d** that were deprotected to obtain compounds **IVa−d** (Scheme 9).

The synthesis of sulfonamide amines **Va−n** was based on the condensation of phthalyl-protected *ω*-aminopentane, aminohexane, and aminoheptane sulfonyl chlorides **XXVa−c** with appropriate amine or hydroxylamine derivatives to produce the corresponding sulfonamides **XXVIa−j,l−n** (Scheme 10). In the case of tertiary sulfonamides **XXVIh,i,l,m**, the synthesis included an extra alkylation step of initially obtained secondary sulfonamides **XXVIIa−c**. The following treatment of the sulfonamides **XXVIa−j,l−n** and **XXVIIc** with hydrazine produced the sulfonamide amines **Va−n**. The intermediate sulfonyl chlorides **XXVa,b** were obtained by a short synthetic sequence from potassium phthalimide **XXII**, including monoalkylation of the latter with 1,5-dibromopentane or 1,6-dibromohexane, treatment of the obtained bromo derivatives **XXIIIa,b** with sodium sulfite, and conversion of the resulting sodium sulfonates **XXIVa,b** into the corresponding sulfonyl chlorides **XXVa,b** with PCl_5. The sulfonyl chloride **XXVc** was obtained using the literature procedure.[40]

SAR. Compounds **1** and **2** (Figure 1) represent two distinct compound classes, which are bioisosters, both targeting the NAMPT enzyme. The common features in the two compounds are the pyridyl head group, a functional group with hydrogen-binding capabilities, a linker chain, and an aromatic group in the end of the linker. With the aim of discovering new compounds with improved activity and toxicological properties, the SAR of these compounds was explored by modification of the mentioned key structural elements (Figure 2).

The primary determination of activity was performed using a WST-1 cell viability and proliferation assay in two cell lines, a breast cancer, MCF-7, and an ovarian carcinoma, A2780. The WST-1 assay determines the metabolic activity of the cells, in a process dependent on NADH as coenzyme; thus, this assay will have a strong functional connection to the NAMPT inhibition.

Modification of Aromatic End Group. Initially, the aromatic end group of compound **2** was modified by preparing novel hydroxamic acid esters that immediately gave potent analogues in the in vitro test system, represented by the first hit compound **4** with nanomolar activity (Table 1 and Figure 3).

In the crystal structure of NAMPT cocrystallized with compound **1**, a rather large binding region near the surface of the protein can be observed where the side chain end group of the ligand is placed.[41] As in earlier work, the published crystal structure of NAMPT cocrystallized with **1** was used as starting point for docking analysis[42] (PDB ID 2GVJ), which was carried out in Glide (further details in the Experimental Section). Previously, we found that different ligands for NAMPT had such similar geometric features that compounds **2** and **5** could even be docked into the crystal structure of compound **1** *without* removing the crystallographic water molecules in the active site.[42] However, due to the much larger and more diverse set of ligands, we chose to completely remove the crystallographic waters in the current study. In the Supporting Information, we have included additional pictures showing the crystal structure with the crystallographic water molecules present, and it is evident that only a few water molecules penetrate the active site when the ligand is present.

When **1** was redocked into the empty active, it achieved the crucial hydrogen bonding to Ser275, albeit with a slightly longer distance (2.3 Å) compared to the 1.8 Å observed in the X-ray structure (Figure 4).

Docking of compound **4** suggested a similar binding mode as compared to **1** (Figure 5) where the cyanoguanidine is capable of achieving a similar hydrogen bond to Ser275. Furthermore, the cyanoguanidine established two new hydrogen bonds to Asp219, which may serve as part of the explanation for the efficiency of this chemical motif.

Scheme 9. Synthesis of Hydroxamate Amines IVa−d

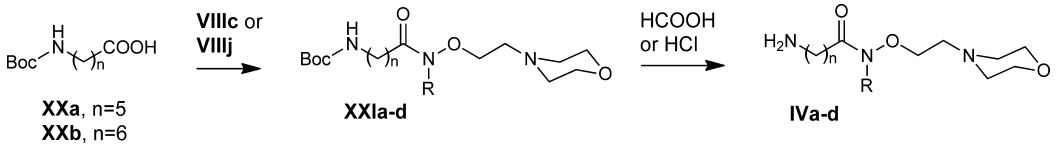

No	n	R
XXIa, IVa	5	Bn
XXIb, IVb	6	Cyclohexyl
XXIc, IVc	7	Bn
XXId, IVd	6	Bn

dx.doi.org/10.1021/jm4009949 | J. Med. Chem. XXXX, XXX, XXX−XXX

Scheme 10. Synthesis of Sulfonamide Amines Va−n

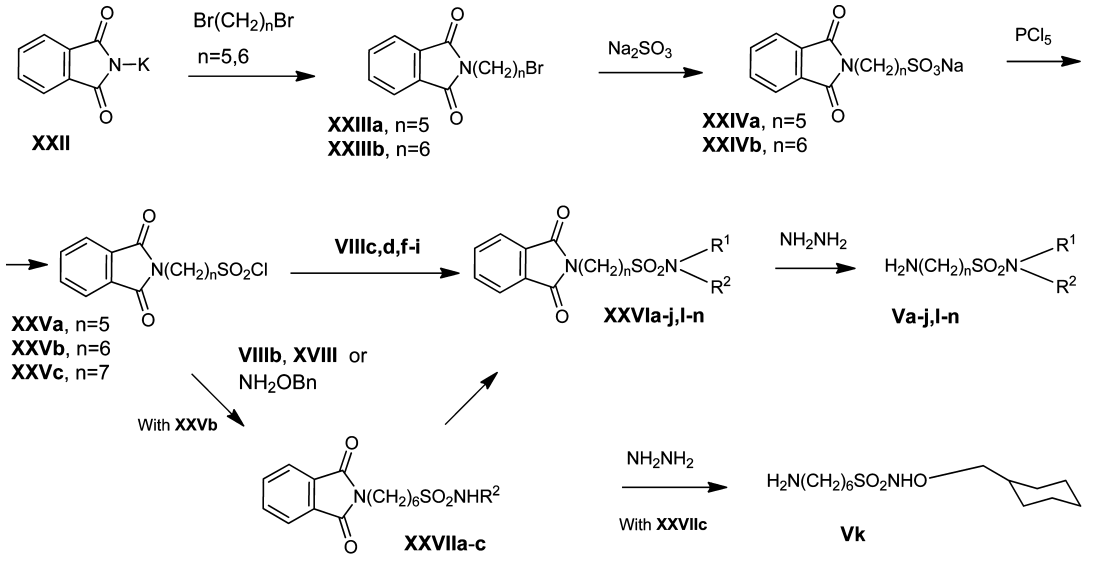

No	n	R^1	R^2
XXVIa, Va	5		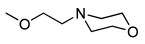
XXVIb, Vb	5		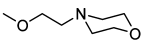
XXVIc, Vc	6		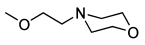
XXVId, Vd	6		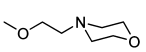
XXVIe, Ve	6		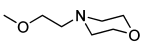
XXVIf, Vf	6		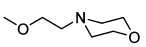
XXVIg, Vg	6		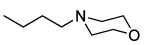

No	n	R^1	R^2
XXVIIb, XXVIh, Vh	6	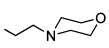	
XXVIIc, XXVIi, Vi	6		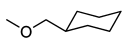
XXVIj, Vj	7		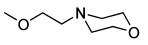
XXVIIa, XXVIl, Vl	6		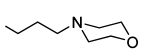
XXVIIc, XXVIm, Vm	6	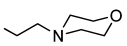	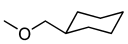
XXVIn, Vn	5		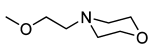

To investigate the preferred binding orientation of the side chain in compound **4**, the close α-methyl and α-benzyl analogues were prepared in an enantiomerically pure form. A stereochemical preference for the (*S*)-methyl derivative (**6**) was found, with a 40 times higher activity, as compared with the (*R*)-methyl derivative (**7**) (Table 2). However, this was not reflected in the calculated docking scores for the interaction that showed a reversed preference. The reasons for this discrepancy were not clear from visual inspection of the docked structures, since they were virtually superimposable in spite of the difference in stereochemistry. Therefore, we speculate that the observed difference in activity could be due to one of several factors that are not accounted for in simple docking calculations such as protein flexibility or different interactions with the hydrogen-bond network between enzyme and water molecules. The similarity in physicochemical properties leads us to believe that the observed difference is not due to differences in pharmacokinetics. The activity difference was very small for the corresponding benzyl enantiomers (**8** and **9**), probably due to the similar size of the binding end groups in the molecule (Table 2). Thus, the docking analysis of these structures did not reveal any obvious differences, or a preferred fit, of the enantiomers with the protein structure. Even though the chiral derivatives were very potent with subnanomolar activity, this compound group was not further explored due to a generally low stability and rapid hydrolysis in mouse plasma (data not shown).

An improvement of both stability and activity was found for the hydroxamic acid esters bearing an additional substituent on the hydroxamic acid nitrogen, compounds **5**, **10**, **11** and **12** all

dx.doi.org/10.1021/jm4009949 | J. Med. Chem. XXXX, XXX, XXX−XXX

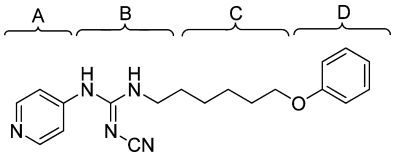

Figure 2. Overview of the sequence of the described SAR work: (1) Modification of aromatic end group D to hydroxamic acid esters (**4**–**12**); (2) SAR for pyridyl head group A (**10** and **13**); (3) SAR of hydrogen-binding group B, replacement of cyanoguanidine with squaric acid and urea (**26**, **28**, **29**, **38**, and **39**); (4) Change of the hydroxamic acid ester for a preferred alkoxy sulphonamide or sulphonamide in D (e.g., **10** vs **15** and **26** vs **31**); (5) Optimization of linker length C and end group for squaric acids (**31**–**34** and **36**) and urea derivatives (**40**–**42** and **44**); (6) Final optimization of the cyanoguanidine series with a pyridyl head group and an alkoxy sulphoneamide (**17** and **20**–**25**).

exhibiting subnanomolar activities (Table 1). From the docked structures, it is clear that these ligands are capable of spanning the wide entrance of the cleft of the protein active site thereby increasing their binding affinities. At the present time, it is unclear whether this increase is due to additional (nonspecific) binding interactions with the protein surface or that the increased binding is caused by a decreased number of accessible conformations of the free ligands.

SAR for Pyridyl Head Group. In earlier studies, the pyridyl head group in the parent compounds has been found essential for high activity.[22] To investigate the importance of the head group in this series, a phenyl derivative, compound **13**, was prepared and found approximately 1000–2000 times less potent as compared with the analogous compound **10** (Table 1). This large difference in activity is difficult to explain since the two head groups (phenyl and pyridine) are both capable of sandwiching between Tyr18 and Phe193 (Figure 6).

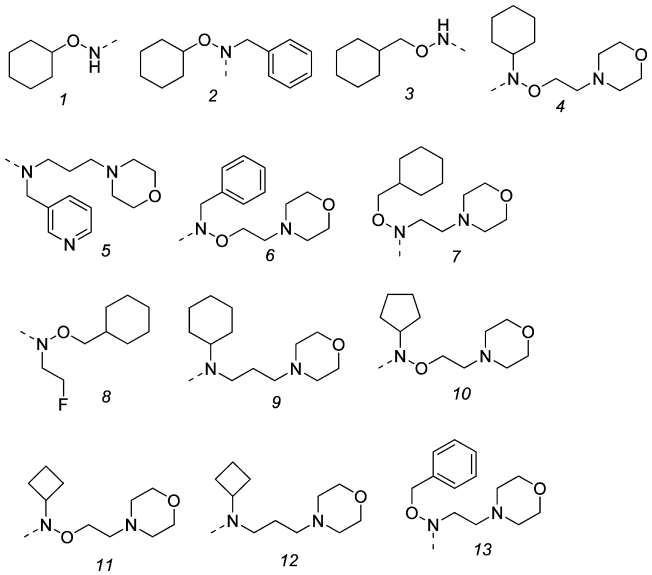

Figure 3. Structures of molecular fragment B in Tables 1, 3, and 4.

To investigate this difference in more detail, we carried out an analysis of the binding energy using density functional theory (DFT) in combination with the B3LYP functional with added dispersion corrections (DFT-d3).

Due to the computational demands of DFT-d3, the enzyme was reduced to an active site model consisting of Arg196, B-

Table 1. NAMPT Inhibitors with a Cyanoguanidine Binding Group

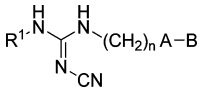

					cell line			
					A2780[a]		MCF-7[a]	
compd	R^1	*n*	A	B[b] structure	IC_{50}, (mean, nM)	SD	IC_{50}, (mean, nM)	SD
1, APO866	–	–	–	–	1.6	±1.5	7.4	±0.68
2, CHS828	–	–	–	–	0.56	±0.19	1.6	±1.3
4	4-pyridyl	6	CO	*1*	35	±13	940	±377
5	4-pyridyl	6	CO	*2*	0.055	±0.036	1	±0.80
10	4-pyridyl	6	CO	*4*	0.1	±0.11	0.42	±0.08
11	4-pyridyl	7	CO	*6*	0.01	±0.014	ND[c]	
12	4-pyridyl	5	CO	*6*	0.081	±0.10	0.021	±0.002
13	phenyl	6	CO	*4*	98	±34	1016	±737
14	4-pyridyl	6	SO_2	*3*	0.16	±0.18	3.4	±2.3
15	4-pyridyl	6	SO_2	*4*	0.025	±0.021	0.33	±0.63
16	3-pyridyl	6	SO_2	*4*	0.51	±0.31	2.9	±1.10
17	4-pyridyl	6	SO_2	*8*	0.052	±0.060	0.1	±0.19
18	4-pyridyl	6	SO_2	*9*	0.16	±0.35	0.11	±0.24
19	4-pyridyl	7	SO_2	*4*	0.089	±0.091	0.29	±0.42
20	4-pyridyl	5	SO_2	*4*	0.011	±0.017	0.036	±0.015
21	4-pyridyl	6	SO_2	*10*	0.0041	±0.0032	ND[c]	
22	4-pyridyl	6	SO_2	*11*	0.049	±0.031	0.007	±0.008
23	4-pyridyl	6	SO_2	*12*	0.091	±0.11	0.1	±0.01
24	4-pyridyl	5	SO_2	*10*	0.022	±0.03	0.041	±0.01
25	4-pyridyl	6	SO_2	*13*	0.053	±0.07	0.63	±0.29

[a]Activities were determined in a WST-1 assay. [b]See Figure 3. [c]ND, not determined.

dx.doi.org/10.1021/jm4009949 | J. Med. Chem. XXXX, XXX, XXX–XXX

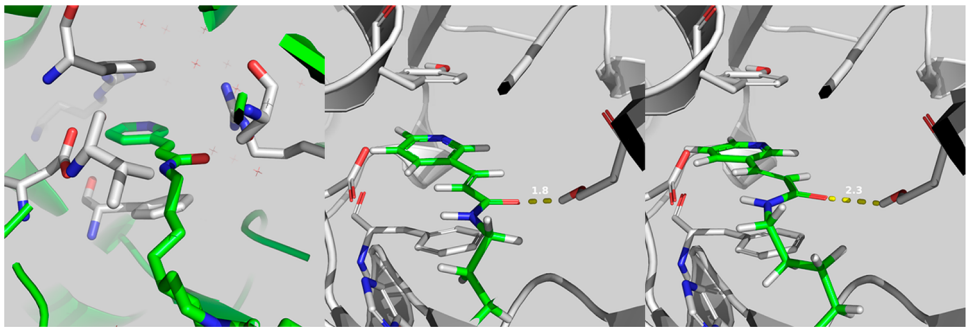

Figure 4. (left) Illustration of **1** docked in the NAMPT X-ray structure (PDB ID 2GVJ). Notice the lack of crystallographic waters in the binding cleft (additional orientations are included in the Supporting Information). (center) Pose of **1** observed in the X-ray with hydrogens added and waters removed. (right) Pose obtained by docking **1** into the "dry" active site of NAMPT.

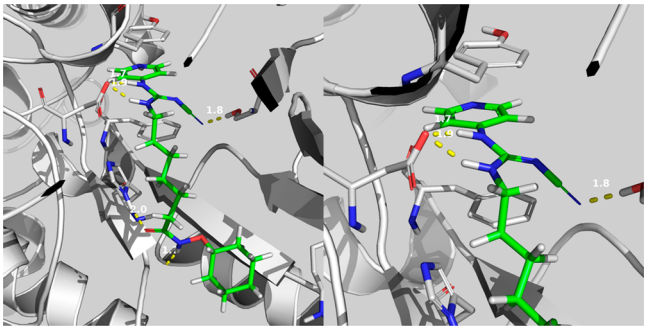

Figure 5. (left) Conformation of **4** docked into the NAMPT active site (PDB ID 2GVJ). (right) Close-up of the pyridine sandwich with the three hydrogen bonds made by the cyanoguanidine moiety.

Table 2. NAMPT Inhibitors with a Chiral End Group

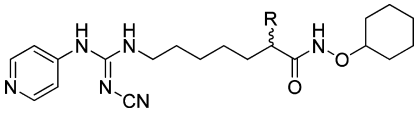

		cell line			
		A2780[a]		MCF-7[a]	
compd	R	IC_{50}, (nM)	SD	IC_{50}, (nM)	SD
6	(*S*)-Me	0.08	ND[b]	1	±0.8
7	(*R*)-Me	3.9	±0.64	38.3	±27.8
8	(*S*)-Bn	0.32	±0.03	5.3	±3.4
9	(*R*)-Bn	0.22	±0.28	1.7	±0.6

[a]Activities were determined in a WST-1 assay. [b]ND, not determined.

chain Tyr18, B-chain Asp16, Asp219, Phe193, Arg311, and Ser275. The amino acids were truncated at the Cα in line with earlier work.[43] Since the aim of the study was primarily to delineate the effect of the head group, it was also decided to truncate the ligands in the spacer region so it consisted of just a single methyl group. A single-point energy calculation shows that the pyridine has an interaction energy that is 22 kJ/mol larger than that for the corresponding structure with a phenyl as the head group, which is in qualitative agreement with the experimental results. In the cyanoguanidine series, the 4-pyridyl head group was compared with the analogues 3-pyridyl derivative, compound **15** versus **16** (Table 1). This comparison showed a greater than 10-fold activity preference for the 4-pyridyl group. A similar activity preference was found for other 4-pyridyl versus 3-pyridyl compound pairs (data not shown), but in this case, the observation could not be explained by the

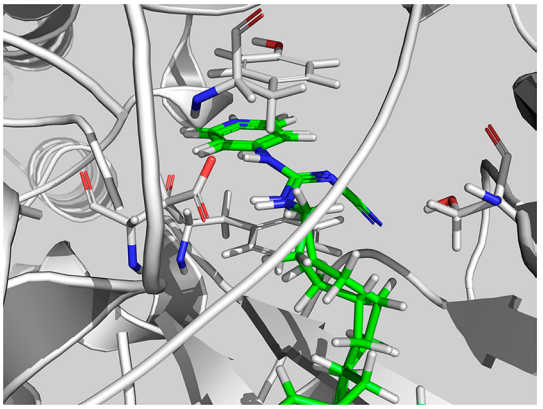

Figure 6. Docking of **10** and **13** in the NAMPT X-ray structure (PDB ID 2GVJ), where it is clear that the head groups are virtually superimposable.

DFT calculations, since 4-pyridyl and 3-pyridyl head groups had a similar stabilization energy (within 1 kJ/mol). At present, it is unclear whether more extended conformational sampling combined with, for example, advanced mixed quantum mechanics/molecular mechanics (QM/MM) calculations could delineate this interesting experimental difference in activity.

SAR of Hydrogen-Binding Group. The next structural modification made was a replacement of the cyanoguanidine with other hydrogen-binding groups. There have been previous attempts to substitute the cyanoguanidine or amide group of compounds **1** and **2** with other groups retaining activity (Figure 1).[28] In this investigation, the most promising substitutions were found to be the squaric acid and urea analogues. The squaric acid compounds **26**, **28**, and **29** (Table 3) and the urea and thiourea derivatives with a 3-picolyl head group, compounds **38** and **39**, respectively (Table 4), both series with a hydroxamic acid ester end group, all were potent inhibitors of proliferation. As expected, docking of these structures showed that they too were capable of obtaining the crucial hydrogen-bonding interactions in the active site of NAMPT (Figure 7).

Squaric acids with similar side chains as the parent compounds **1** and **2** have been reported in the patent literature to have antiproliferative activity.[44] This finding suggests a further exploration of the squaric acid bioisosters with novel side chains.

Change of the Hydroxamic Acid Ester. With three structural core elements in hand, the cyanoguanidine, the

dx.doi.org/10.1021/jm4009949 | J. Med. Chem. XXXX, XXX, XXX−XXX

Table 3. NAMPT Inhibitors with a Squaric Acid Binding Group

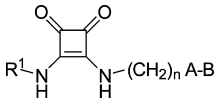

					cell line			
					A2780[a]		MCF-7[a]	
compd	R^1	*n*	A	B[b] structure	IC_{50}, (mean, nM)	SD	IC_{50}, mean, (nM)	SD
26	4-pyridyl	6	CO	*4*	0.03	±0.02	ND[c]	
27	4-pyridyl	6	SO_2	*5*	4.1	±2.2	21.6	±4.5
28	4-pyridyl	6	CO	*6*	0.29	±0.32	12.3	±5.0
29	4-pyridyl	5	CO	*6*	0.68	±0.47	23	±1.1
30	4-pyridyl	6	SO_2	*7*	0.73	±0.03	10.8	±2.3
31	4-pyridyl	6	SO_2	*4*	0.49	±0.22	9	±2.9
32	4-pyridyl	7	SO_2	*4*	0.49	±0.17	8	±5.2
33	4-pyridyl	5	SO_2	*4*	0.57	±0.12	35.8	±8.4
34	4-pyridyl	6	SO_2	*10*	0.59	±0.35	13.7	±2.4
35	4-pyridyl	6	SO_2	*11*	0.2	±0.14	29.1	±6.4
36	4-pyridyl	5	SO_2	*10*	0.38	±0.05	46.3	±6.3

[a]Activities were determined in a WST-1 assay. [b]See Figure 3. [c]ND, not determined.

Table 4. NAMPT Inhibitors with a Urea (Thiourea) Binding Group

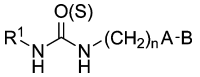

					cell line			
					A2780[a]		MCF-7[a]	
compd	R^1	*n*	A	B[b] structure	IC_{50}, (mean, nM)	SD	IC_{50}, (mean, nM)	SD
37	4-pyridyl	6	SO_2	*4*	0.25	±0.13	0.05	±0.01
38	3-picolyl	6	CO	*4*	0.27	±0.13	0.37	±0.51
39	3-picolyl[c]	6	CO	*4*	0.91	±0.31	5.5	±2.2
40	4-pyridyl	6	SO_2	*7*	0.56	±0.01	1.4	±0.05
41	3-picolyl	6	SO_2	*7*	0.17	±0.06	0.93	±0.11
42	4-pyridyl	5	SO_2	*4*	3.4	±2.2	28	±11.2
43	4-pyridyl	7	SO_2	*4*	1.8	±0.07	7.4	±4.6
44	3-picolyl	5	SO_2	*4*	4.6	±4.5	6.5	±5.7
45	3-picolyl	7	SO_2	*4*	0.31	±0.11	3.6	±2.3
46	3-picolyl	6	SO_2	*10*	0.58	±0.18	5.8	±0.15
47	3-picolyl	6	SO_2	*11*	2.2	±0.12	11	±5.0
48	3-picolyl	6	SO_2	*12*	1.7	±0.21	8.7	±7.2
49	3-picolyl	5	SO_2	*11*	13	±6.4	49	±33.7
50	3-picolyl	5	SO_2	*10*	2.7	±1.9	7	±1.2
51	4-pyridyl[c]	6	SO_2	*10*	0.16	±0.15	0.31	±0.40

[a]Activities were determined in a WST-1 assay. [b]See Figure 3. [c]The compound is a thiourea.

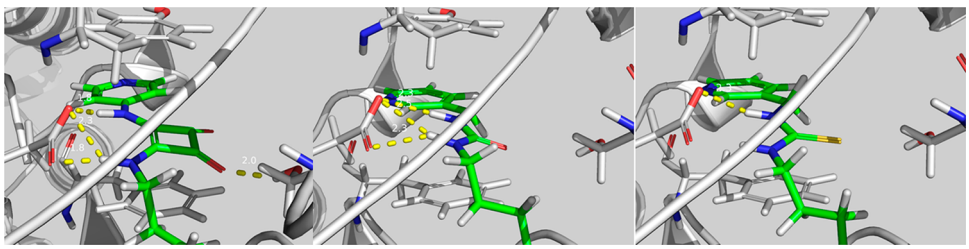

Figure 7. Compounds docked in the NAMPT X-ray structure (PDB ID 2GVJ). (left) **26**, a representative of the squaric acid series with dotted lines indicating the hydrogen bonds made to Ser275 and Asp219. (center) **38**, the urea linker also allows hydrogen bonds to be made to Asp219. (right) **39**, also the larger thiourea can be accommodated in the active site.

squaric acid, and the urea, all producing highly active compounds, a further optimization was structured. Changing the hydroxamic acid ester for an alkoxy sulphonamide or sulphonamide gave a more robust series of compounds with high activity, and this substitution was used in the further SAR work (see e.g., **10** vs **15**, Table 1 and **26** vs **31**, Table 3).

dx.doi.org/10.1021/jm4009949 | J. Med. Chem. XXXX, XXX, XXX−XXX

Squaric Acid Series. In the squaric acid series, compounds **31**, **34**, and **35** were prepared to explore the effect of ring size in the end group; however, no significant difference in binding affinity/antiproliferative activity was found (Table 3). This is understandable also from the docking results, since the head groups dock in a similar position in the active site, as expected (Figure 8, left), whereas the flexible end of the chain can freely position itself in the wide entrance region of the catalytic cleft.

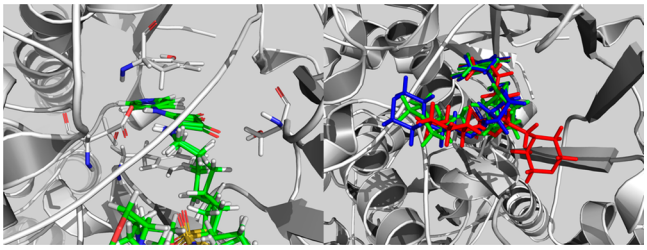

Figure 8. Compounds docked in the NAMPT X-ray structure (PDB ID 2GVJ). (left) Compounds **31**, **34**, and **35** all dock into the sandwich region of the enzyme. (right) Wide entrance region allows the ligands to obtain different positions that do not offer any differences in activity between compounds having a five-membered (green), six-membered (red), or four-membered rings (blue) as substituent on nitrogen.

Likewise, the linker length was varied from five to seven carbons in compounds **31**–**33** and **34** versus **36** that gave compounds with similar activity, however with a slight activity preference for compounds with six carbons in the linker (Table 3). Shorter and longer linker chains gave compounds with lower antiproliferative activity (data not shown).

For compounds **31**–**33**, the docking analysis shows a preference for a hydrogen-bond interaction between the sulphonamide moiety and His191. This enforces a constraint on the length between the sulphonamide and the pyridine head group, which is suitable for a six-carbon linker (**31**). The docking results showed that the shorter chain introduces strain in the structure (**33**) and the longer seven-carbon linker has to coil up to satisfy the distance requirement (**32**). However, we should stress that the similarity in the biological activity shows that such accommodation is possible and indeed takes place without significant loss in activity.

The squaric acid **27**, a sulphone amide, was less active; however, this compound was not strictly analogous to any alkoxy sulphone amide, since it has an additional pyridine group in the end group of the molecule. In all three series, the sulphonamide end groups were found equipotent or slightly less potent as compared with similar alkoxy sulphonamide (see compounds **18**, **23**, **27**, and **48**, Tables 1–4).

Urea Series. The urea derivatives were designed as analogues to compound **1** where the unsaturated amide was replaced by a urea group. In this series, compounds with a 4-pyridyl or a 3-picolyl head group were compared, compounds **40** versus **41** and **42** versus **44**, and found equipotent despite the structural difference in the head group (Table 4). Computational modeling of these interactions showed that, despite the difference in the location of the pyridine nitrogen, the aromatic group positions itself perfectly aligned in the pocket between Tyr18 and Phe193. This introduces a slight difference in the orientation of the urea moiety but does not hinder the formation of hydrogen bonds to Asp219. As mentioned earlier, our simple DFT model of the binding site does not reveal any differences in the $\pi-\pi$ stacking ability of the two head groups, which is in line with the observation for the urea series.

Similar to the squaric acid analogues, a linker of five to six carbons gave highly active compounds both with a pyridyl head group (**37**, **42**, **43**) and a picolyl head group (**46**, **47**, **49**, **50**, Table 4).

Also in the urea series, many of the analogues showed subnanomolar activities either with a pyridyl or picolyl head group, a urea or thio-urea binding group, and a series of different end groupings.

Cyanoguanidine Series. Returning to the cyanoguanidine series with a pyridyl head group and an alkoxy sulphone amide connecting the linker and end groups, the most potent compounds with low picomolar antiproliferative activity, for example, compounds **17** and **20**–**25**, were found (Table 1). Similar to the other series, a linker of six carbons was optimal.

In summary, using a functional cell proliferation assay, a rather broad SAR was determined. Highly active compounds were found in all three series, the cyanoguanidine, the squaric acid, and the urea series, suggesting an analogous interaction with the target NAMPT enzyme. Also, a similar substitution pattern was used to obtain the most potent compounds in the three series suggesting a similar binding to the target.

IN VITRO ACTIVITY AND MODE OF ACTION

To further characterize the key compounds, the IC_{50} values of a number of them were established in the colon cancer cell line HCT-116 and a derived compound **1** resistant cell line HCT-116/APO866 (Table 5). Determination of the actual sensitivity of the cell line with acquired resistance was not possible. However, the resistance toward the compounds was at least 128–2632-fold higher in HCT-116/APO866 compared to the parental cell line. The mechanism of resistance in HCT-116/APO866 has been determined to be specifically due to a mutation, H191R, in the active site of NAMPT that results in highly specific resistance.[29,42] Thus, the high level of cross-resistance observed for the compounds in this study strongly suggests that their mechanism of action likewise is through inhibiting NAMPT and thus similar to that of compound **1**.

Table 5. IC_{50} Values for Key Compounds for Antiproliferative Effects in HCT-116 and Compound 1 Resistant HCT-116/APO Cells

	cell line		
	HCT-116[a]		HCT-116/APO866[a]
compd	IC_{50} (nM)	±SD	IC_{50} (nM)
1	10.9	6.1	946
15	1,9	0,2	>5000
17	3,6	2,4	>5000
31	39	13	>5000
37	5,3	2,9	>5000

[a]Activities were determined in a WST-1 assay.

In order to confirm the on-target mechanism of action for the new series of compounds, the enzyme inhibitory activity was determined using a NAMPT enzymatic assay with HepG2 lysates as the source of NAMPT enzyme (Table 6). Even though the correlation with the antiproliferative activity data was not perfect, all tested compounds showed high potency with low nanomolar activity, which is a strong support for a

dx.doi.org/10.1021/jm4009949 | J. Med. Chem. XXXX, XXX, XXX–XXX

Table 6. NAMPT Enzyme Assay (IC_{50}, nM)

	compd								
	1	**2**	**4**	**5**	**10**	**11**	**14**	**15**	**17**
IC_{50} (nM)	2.2	18.3	1.1	38.5	0.2	4.4	2.4	0.3	3.2

	compd							
	18	**27**	**32**	**33**	**37**	**39**	**40**	**41**
IC_{50} (nM)	2.4	22.8	3.6	49.6	49	8.2	133.2	11.8

direct enzyme interaction. The discrepancy between enzyme inhibition and antiproliferative activity is suggested to be due to the different properties of the compounds such as cell penetration that is important in the cellular assay. Compounds were selected for further testing primarily based on in vitro activity but also to cover the chemical classes. Key compounds were also characterized in a clonogenic assay in several cancer cell lines (Table 7). Compounds **15** and **17** showed similar or increased potency in these assays as compared to reference compound **1** and were thus selected for further in vivo characterization.

Table 7. Clonogenic Assay for Compounds 15, 17, and 1 in a Selection of Cancer Cell Lines

	compd		
cell line	**15**, IC_{50} (nM)	**17**, IC_{50} (nM)	**1**, IC_{50} (nM)
A2780	0.55 (24 h)	0.43 (16 h)	5.7
A431	>50	ND[a]	6.1
DU145	>50	6.39	ND[a]
MCF-7	>50 (24 h)	>50 (24 h)	8.4
	1.9 (96 h)	0.98 (96 h)	ND[a]
NYH	0.3	0.05	1.5
PC-3	0.53	0.35	3.8
SK-OV-3	9.9	3.4	211

[a]ND, not determined.

In Vivo Antitumor Activity. Compounds with potent (nM) activity from all series were taken forward to tests of pharmacokinetics and preliminary toxicology effects in mouse as a selection filter for in vivo test in an A2780 xenograft mouse model (Table 8). Several of the new compounds compared well with the reference compound **1**, and on the basis of these data, compounds were selected. Most compounds in these series exhibited a relatively short half-life, approximately 20 min, but with an adequate systemic exposure (AUC).Therefore, in this early screen for pharmacological activity in vivo, the compounds were administered ip to secure a sufficient exposure of the compound in the animal.

Treatment with compound **17** (15 mg/kg bid ip for 10 consecutive days (small tumors) or two 5 day cycles (large tumors) had good therapeutic effect in both small and large A2780 tumors (Figure 9). A clear decrease was seen in the

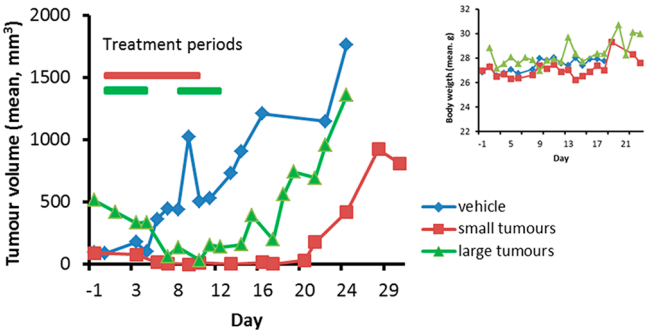

Figure 9. Tumor growth curves of compound **17** in an A2780 xenograft mouse model. 15 mg/kg bid ip on days 0–4 and 7–11 (large tumors; starting volume 500 mm^3) or days 0–9 (small tumors; starting volume 100 mm^3). Inserted graph: body weight change during treatment.

tumor volumes during the treatment period, and some mice even showed a transient cure and eradication of the tumor. After treatment, the tumors resumed growth at various time points and grew to the maximum allowed size (1000 mm^3). Treatment with compound **17**, 15 mg/kg, using the schedules above was well tolerated and did not affect the body weight as compared with vehicle-treated animals (Figure 9, insert).

Similarly, compound **15** was tested in the A2780 xenograft model with large tumors (3 mg/kg, ip, bid, 10 consecutive days) (Figure 10). Compound **15** showed good efficacy, and on average, treatment reduced the tumor volume significantly to one-fifth of the volume from start of treatment (Figure 10A).This dose was found well tolerated in the mice (Figure 10C). Compound **15** was tested at higher doses (5 and 10 mg/kg) with very clear therapeutic effects; however, already at 5 mg/kg, four of nine mice showed toxic signs in the form of body weight loss and reduced activity level as compared to the control that was further accentuated at 10 mg/kg (data not shown). Thus, it was concluded that a 3 mg/kg bid dose was at the MTD level for compound **15**, in this model.

In a comparative study with these two compounds (**15** and **17**) and the reference compound **1**, compound **15** was found approximately 12 times more potent than **1** in the A2780 xenograft mouse model (schedule: ip bid day 0–4, starting tumor volume 100 mm^3) as measured by the tumor volume at day 14. Significant reduction of A2780 tumor volume at day 14 was observed after treatment with compound **15**, 1.25 and 2.5

Table 8. Toxicological and Pharmacokinetic Data for Selected Derivatives as Determined in Mouse

	toxicology[a]			pharmacokinetics					
compd	MTD (mg/kg)	dose for PK (mg/kg)	route	$t^1/_2$ (h)	t_{max} (h)	C_{max} (ng/mL)	V_x (mL/kg)	CL (mL/(h·kg))	AUC ((h·ng)/mL)
1	10 < MTD < 50	20	iv	0.4	0.25	14 563	998	1620	12 337
15	MTD < 10	50	iv	0.18	0.08	14 102	1275	4906	10 184
17	10 < MTD < 50	50	iv	0.36	0.08	78 519	547	1052	47 514
31	10 < MTD < 50	50	iv	0.21	0.083	33 535	1200	3995	12 499
37	MTD < 10	50	iv	0.45	0.08	14 827	4600	7105	7018

[a]The compound toxicity (MTD) was estimated in NMRI mice dosing the compounds bid ip for five consecutive days, determining weight loss and blood cell counts.

dx.doi.org/10.1021/jm4009949 | J. Med. Chem. XXXX, XXX, XXX–XXX

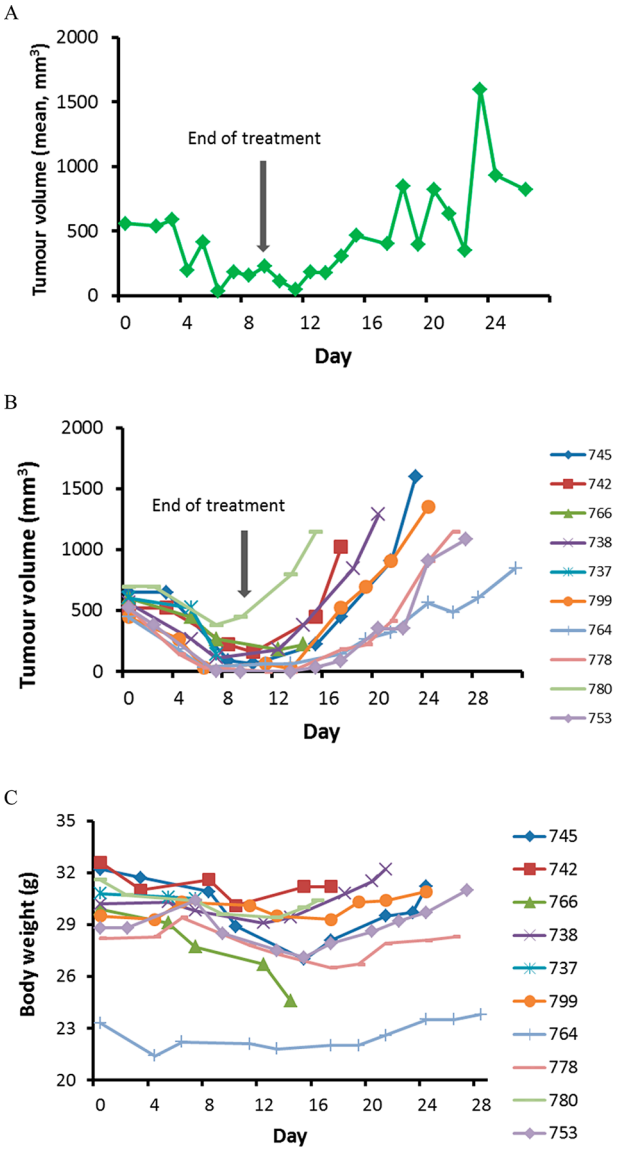

Figure 10. Treatment with compound **15** in an A2780 xenograft mouse model (large tumors, 3 mg/kg, ip, bid). (A) Mean tumor volume; (B) tumor volume in individual mice; (C) body weight during treatment in individual mice.

mg/kg, and compound **1**, 15 mg/kg. A dose−response effect of **15**, 0.63, 1.25, and 2.5 mg/kg, was observed with percent volume of treated tumors versus control T/C% of 82%, 40%, and 24%, respectively. Also, some effect (T/C = 52%), however not significant, was determined after treatment with compound **17** and compound **1** (Figure 11). Critical body weight losses were not observed in any treatment groups.

In summary, in vivo the selected compounds showed an equal or increased potency as compared with reference compound **1**, with no critical signs of toxicology using effective doses. These highly promising results suggest a continuation of studies of this compound class.

CONCLUSION

The present study describes the successful discovery of novel NAMPT inhibitors with promising biological activities as antiproliferative agents in cancer cell lines in vitro and potent tumor reduction efficacy in vivo in a xenograft mouse model.

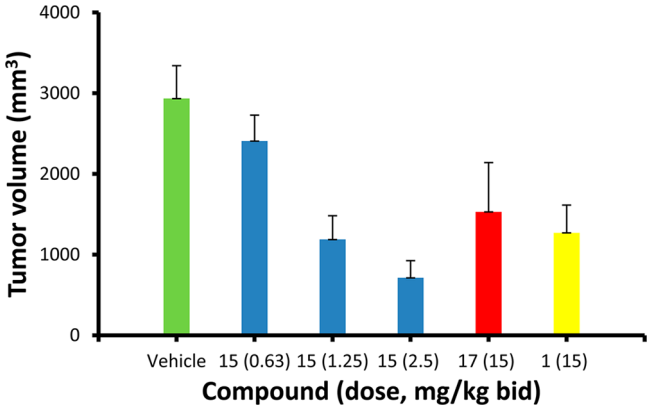

Figure 11. Tumor volume at day 14 after treatment with compounds **15** (0.63, 1.25, 2.5 mg/kg), **17** (15 mg/kg), and **1** (15 mg/kg) bid day 0−4 as compared with vehicle, in a A2780 xenograft mouse model.

The structure-based method used for the optimization of these structures gave a rationale for the obtained activities and knowledge about the scope and limitation in the design of new NAMPT inhibitors. The most active compounds in these new series compared favorably, in respect to toxicology and in vivo activity, with compounds already in the clinic and warrant further investigation as promising lead molecules for the inhibition of NAMPT.

EXPERIMENTAL SECTION

Reaction conditions and yields were not optimized. ^{1}H and ^{13}C NMR spectra were recorded on a Bruker Avance 300 spectrometer (300 MHz) or Varian 400 OXFORD NMR spectrometer (400 MHz). Chemical shifts are reported in parts per million (δ) and referenced to hexamethyldisiloxane (HMDSO) as an internal standard or using the signal according to deuterated solvent for ^{1}H spectra ($CDCl_3$, 7.26; CD_3OD, 3.31; $(CD_3)_2SO$, 2.50) and ^{13}C spectra ($CDCl_3$, 77.23; CD_3OD, 49.00; $(CD_3)_2SO$, 39.52). The value of a multiplet, either defined (doublet (d), triplet (t), double doublet (dd), double triplet (dt), quartet (q)) or not (m) at the approximate midpoint is given unless a range is quoted. A broad singlet is indicated by "bs". Mass spectrometry (MS) was performed using an LC-MS using a Bruker Esquire 3000+ ESI ion-trap with an Agilent 1200 HPLC-system or on an Acquity UPLC system (Waters) connected to the Micromass Q-TOF micro hybrid quadrupole time-of-flight mass spectrometer operating in the electrospray ionization (ESI) positive ion mode and using a reverse-phase Acquity UPLC BEH C18 column (1.7 μm, 2.1 mm × 50 mm) on a gradient of 5−98% acetonitrile−water 0.1% formic acid. All tested compounds were of sufficient purity (>95%) as determined by high-performance liquid chromatography (HPLC), using an Agilent 1200 HPLC system. High-resolution MS (HRMS) was carried out on a Micromass Q-Tof micro mass spectrometer. Elemental analyses were performed on Carlo Erba CHNS-O EA-1108 apparatus. Melting points were measured on a "Boetius" or Gallenkamp melting point apparatus and are uncorrected. Silica gel, 0.035 e 0.070 mm, (Acros) was employed for column chromatography.

Preparation of Key Compounds 15 and 17. For a full description of the preparation and spectroscopic data of compounds reported in this paper please see the Supporting Information.

*6-(2-Cyano-3-(pyridin-4-yl)guanidino)-N-cyclohexyl-N-(2-morpholinoethoxy)hexane-1-sulfonamide (**15**). 2-(2-Morpholinoethoxy)isoindoline-1,3-dione (**XIVc**).* Synthesis of compound **XIVc** by a modified version of published procedures[45−47] was performed as follows: To a mixture of 2-hydroxyisoindoline-1,3-dione (33.92 g, 208 mmol) and 4-(2-chloroethyl)morpholine hydrochloride (50.24 g, 270 mmol) in 1-methyl-2-pyrrolidinone (160 mL) slowly was added DBU (80 mL, 535 mmol), and the resulting mixture was

dx.doi.org/10.1021/jm4009949 | J. Med. Chem. XXXX, XXX, XXX−XXX

stirred at 45 °C for 6 h. The mixture was poured into water (500 mL) and extracted with ethyl acetate (3 × 250 mL), and the combined extract was washed with brine (200 mL) and dried (Na_2SO_4). The solvent was evaporated, and the residue was dried in vacuo to give compound **XIVc** (39.0 g, 68%) as an oil that solidified on standing. ^{1}H NMR (200 MHz, $CDCl_3$) δ 2.50 (m, 4H), 2.79 (t, J = 5.5 Hz, 2H), 3.59 (m, 4H), 4.37 (t, J = 5.5 Hz, 2H), 7.70−7.89 (m, 4H).

*O-(2-Morpholinoethyl)hydroxylamine (**VIIIe**).* To a solution of 2-(2-morpholinoethoxy)isoindoline-1,3-dione (**XIVc**) (39.0 g, 141 mmol) in a mixture of methanol (200 mL) and dichloromethane (100 mL) was added hydrazine hydrate (20 mL, 411 mmol), and the obtained mixture was stirred at room temperature overnight. The resulting precipitate was filtered off, and the filtrate was concentrated in vacuo. The residue (22.9 g) was mixed with water (200 mL), to this mixture was added conc. HCl (30 mL), and the solid material was filtered off. The filtrate was washed with EtOAc (200 mL), and the pH of the medium was raised to 10 by adding 5 N aqueous NaOH. The mixture was extracted with chloroform (3 × 300 mL), and the extract was washed with brine (100 mL) and dried (Na_2SO_4). The solvent was evaporated, and the residue was dried in vacuo to give *O*-(2-morpholinoethyl)hydroxylamine (**VIIIe**) (20.7 g, quantitative yield). ^{1}H NMR (200 MHz, $CDCl_3$) δ 2.44−2.55 (m, 4H), 2.59 (t, J = 5.4 Hz, 2H), 3.69−3.77 (m, 4H), 3.81 (t, J = 5.4 Hz, 2H), 5.50 (b s, 2H).

*Cyclohexanone O-(2-morpholin-4-ylethyl)oxime (**XIXd**).* To a stirred solution of cyclohexanone oxime (**XVIIc**) (22.64 g, 0.2 mol) in dimethylformamide (200 mL) at ice-bath temperature, 60% sodium hydride in mineral oil (16.0 g, 0.4 mol) was added portion-wise, and the resulting mixture was stirred at this temperature for 1 h. To the reaction mixture was added a suspension of 4-(2-chloroethyl)-morpholine (37.22 g, 0.2 mol) in dimethylformamide (100 mL). The ice-bath was removed, and the reaction mixture was stirred at room temperature for 16 h and at 60 °C for 3 h. The mixture was allowed to cool to room temperature and then filtered, and the filtrate was evaporated. The residue was mixed with a saturated ammonium chloride solution in water (300 mL) and extracted with diethyl ether (3 × 200 mL). The combined organic extracts were washed successively with 0.5 N sodium hydroxide (200 mL), brine (200 mL), and dried (Na_2SO_4). The solvent was evaporated, and the residue (36.47 g) was chromatographed on silica gel (250 g) with chloroform−methanol (40:1) as eluent to give compound **XIXd** (35.1 g, 77.5%) as a yellow oil. ^{1}H NMR (400 MHz, $CDCl_3$) δ 1.54−1.71 (m, 6H), 2.18 (m, 2H), 2.43 (m, 2H), 2.52 (m, 4H), 2.66 (t, 2H, J = 5.8 Hz), 3.71 (m, 4H), 4.15 (t, 2H, J = 5.8 Hz).

*4-{2-[(Cyclohexylamino)oxy]ethyl}morpholine (**VIIIc**).* To a solution of cyclohexanone *O*-(2-morpholin-4-ylethyl)oxime (**XIXd**) (13.9 g, 61.4 mmol) in methanol (100 mL) at ice-bath temperature were added sodium cyanoborohydride (7.72 g, 122.8 mmol) and trace of Methyl Orange. To the obtained slightly yellow solution, slowly 2 N HCl solution in methanol was added until the color of the reaction mixture changed from yellow to pink (in about 15 min). The reaction mixture was stirred at room temperature for 5 h, and the solvent was evaporated. To the residue was added water (30 mL), and the pH of the obtained solution was raised to a pH value greater than 9 with 6 N KOH, saturated with sodium chloride. The obtained mixture was extracted with chloroform (3 × 150 mL), and the combined organic extract was washed with brine (100 mL) and dried (Na_2SO_4). The solvent was removed, and the residue was dried in vacuo to afford title compound **VIIIc** (13.0 g, 92%) as a yellow oil. ^{1}H NMR (400 MHz, $CDCl_3$) δ 1.00−1.33 (m, 5H), 1.62 (m, 1H), 1.73 (m, 2H), 1.84 (m, 2H), 2.48 (m, 4H), 2.56 (t, 2H, J = 5.7 Hz), 2.84 (tt, 1H, J = 3.7, 10.5 Hz), 3.71 (m, 4H), 3.81 (t, 2H, J = 5.7 Hz), 5.43 (br s, 1H). LCMS (ESI) m/z: 299 $[M + H]^+$.

*Sodium 6-(1,3-Dioxo-1,3-dihydro-2H-isoindol-2-yl)-1-hexanesulfonate (**XXIVb**).* To a hot solution of 2-(6-bromohexyl)-1*H*-isoindole-1,3(2*H*)-dione (**XXIIIb**)[48] (12.67 g, 40.8 mmol) in ethanol (82 mL) was added a solution of sodium sulfite (10.3 g, 81.7 mmol) in water (80 mL), and the resulting mixture was refluxed overnight. The hot mixture was filtrated, crystallized from ethanol, and dried in vacuo over P_2O_5 to give compound **XXIVb** (8.43 g, 62%). ^{1}H NMR (200 MHz, $(CD_3)_2SO$) δ 1.16−1.41 (m, 4H), 1.41−1.68 (m, 4H), 2.37 (m, 2H), 3.56 (t, 2H, J = 7.0 Hz), 7.77−7.92 (m, 4H). LCMS (ESI): m/z 312 $[M_{sulfonic\ acid} + H]^+$.

*6-(1,3-Dioxo-1,3-dihydro-isoindol-2-yl)-hexanesulfonyl chloride (**XXVb**).* A mixture of sodium 6-(1,3-dioxo-1,3-dihydro-2*H*-isoindol-2-yl)-1-hexanesulfonate (**XXIVb**) (13.99 g, 42.0 mmol) and phosphorus pentachloride (28.0 g, 134.5 mmol) was carefully ground in a mortar (*Caution: a good hood has to be used!*). An evaluation of some amount of gas was observed, and gradually (in 2−3 min), the solid mixture turned into an oily liquid. The obtained liquid was mixed with toluene (280 mL), the precipitated solid material was filtered off and washed with toluene, and the filtrates were combined. The solvent was evaporated, and the residue was azeotropically dried several times with toluene. The obtained white solid was dissolved in ethyl acetate (300 mL), washed successively with water (100 mL), saturated sodium bicarbonate (2 × 100 mL), and brine (2 × 100 mL), and dried (Na_2SO_4). The solvent was evaporated, and the residue was dried in vacuo over P_2O_5 to afford compound **XXVb** (10.4 g, 75%) as white crystals. mp 73−75 °C. ^{1}H NMR (400 MHz, $CDCl_3$) δ 1.41 (qui, 2H, J = 7.6 Hz), 1.55 (qui, 2H, J = 7.6 Hz), 1.72 (qui, 2H, J = 7.4 Hz), 2.04 (m, 2H); 3.65 (m, 2H); 3.69 (t, 2H, J = 7.1 Hz); 7.67−7.75 (m, 2H); 7.80−7.87 (m, 2H). Anal. calcd. for $C_{14}H_{16}ClNO_4S$: C, 50.99; H, 4.89; N, 4.25; S, 9.72. Found: C, 51.03; H, 5.01; N, 4.17; S, 9.68.

*N-Cyclohexyl-6-(1,3-dioxo-1,3-dihydro-2H-isoindol-2-yl)-N-(2-morpholinoethoxy)-1-hexanesulfonamide (**XXVIe**).* A solution of *N*-cyclohexyl-*O*-(2-morpholin-4-yl-ethyl)-hydroxylamine (**VIIIc**) (12.56 g, 55 mmol) and triethylamine (14.0 mL, 100 mmol) in dry dichloromethane (100 mL) under argon atmosphere was cooled to −20 °C. To the stirred solution slowly during 1 h was added a solution of 6-(1,3-dioxo-1,3-dihydro-2*H*-isoindol-2-yl)hexane-1-sulfonyl chloride (**XXVb**) (16.49 g, 50 mmol) in dichloromethane (50 mL), and the resulting mixture was stirred at −20 °C for 20 h. The reaction mixture was concentrated to a small volume and filtered, and the precipitated solid material was washed with dichloromethane. The filtrate was evaporated, and the residue (32.25 g) was dissolved in a small volume of chloroform and chromatographed on silica gel (450 g) with hexane−isopropanol (gradient from 7:3 to 6:4) as eluent. The eluate, containing pure product by thin layer chromatography (TLC), was separated, and the impure material was rechromatographed using the same eluent. The eluates with TLC pure material were combined, the solvent was evaporated, and the residue was dried in vacuo to afford compound **XXVIe** (16.4 g, 62.8%) as a crystalline solid. ^{1}H NMR (400 MHz, $CDCl_3$) δ 1.10 (tq, 1H, J = 3.5, 12.9 Hz), 1.20−1.44 (m, 4H), 1.44−1.76 (m, 7H), 1.76−1.95 (m, 6H), 2.49 (m, 4H), 2.58 (t, 2H, J = 5.6 Hz), 3.08 (bs, 2H); 3.58 (tt, 1H, J = 3.6, 11.7 Hz), 3.68 (t, 2H, J = 7.0 Hz), 3.69 (m, 4H), 4.12 (bs, 2H), 7.71 (m, 2H), 7.83 (m, 2H).

*6-Amino-N-cyclohexyl-N-(2-morpholinoethoxy)-1-hexanesulfonamide (**Ve**).* *N*-Cyclohexyl-6-(1,3-dioxo-1,3-dihydro-2*H*-isoindol-2-yl)-*N*-(2-morpholinoethoxy)-1-hexanesulfonamide (**XXVIe**) (17.608 g, 33.75 mmol) was dissolved in a mixture of chloroform (150 mL) and absolute ethanol (150 mL), and hydrazine hydrate (4.2 mL, 86.54 mmol) was added. The obtained mixture was refluxed for 5 h and then stirred at room temperature overnight. The mixture was filtered, the precipitate was washed with dichloromethane, and the combined filtrates were evaporated. The residue was dissolved in dichloromethane (50 mL), and the mixture was kept in a refrigerator (~5 °C) for 1 h and then filtered again. The filtrate was evaporated, and the residue (14.392 g) was chromatographed on silica gel (200 g) with methanol−30% ammonium hydroxide aqueous solution (gradient from 25:1 to 20:1) to give 8.38 g of an oil. The oil was dissolved in dichloromethane (100 mL), washed successively with water (2 × 20 mL) and brine (20 mL), and dried (Na_2SO_4). The solvent was evaporated, and the residue was dried in vacuo at 50 °C to give compound **Ve** (7.67 g, 63.8%) as a yellow oil. ^{1}H NMR (400 MHz, $CDCl_3$) δ 1.10 (tq, 1H, J = 3.4, 12.9 Hz), 1.20−1.52 (m, 8H), 1.52−1.69 (m, 5H), 1.75−1.98 (m, 6H), 2.49 (m, 4H), 2.59 (t, 2H, J = 5.6 Hz), 2.70 (t, 2H, J = 6.8 Hz), 3.09 (bs, 2H), 3.59 (tt, 1H, J = 3.6, 11.7 Hz), 3.69 (m, 4H), 4.12 (b s, 2H). LCMS (ESI) m/z: 392 $[M + H]^+$. Anal. calcd. for $C_{18}H_{37}N_3O_4S{\cdot}0.15\ H_2O$: C, 54.83; H, 9.54; N, 10.66; S, 8.13. Found: C, 54.86; H, 9.66; N, 10.63; S, 8.14.

dx.doi.org/10.1021/jm4009949 | J. Med. Chem. XXXX, XXX, XXX−XXX

*6-(2-Cyano-3-(pyridin-4-yl)guanidino)-N-cyclohexyl-N-(2-morpholinoethoxy)hexane-1-sulfonamide (**15**).* A mixture of 6-amino-*N*-cyclohexyl-*N*-(2-morpholinoethoxy)-1-hexanesulfonamide (**Ve**) (2.49 g, 6.4 mmol), 4-[(cyanoimino)(methylsulfanyl)methyl]-aminopyridine (**IIIa**) (1.22 g, 6.3 mmol), triethylamine (3 mL, 21.6 mmol), and 4-dimethylaminopyridine (0.1 g, 0.8 mmol) in dry pyridine (4 mL) was stirred at 75−80 °C for 5 h. The solvent was evaporated to dryness, and the residue was chromatographed on silica gel (150 g) with acetonitrile−water (10:1) as eluent to give compound **15** (1.8 g, 53%) as a foam together with a less pure material (1.0 g, 29%) that can be purified repeatedly by column chromatography to increase the yield of the process. ^{1}H NMR (200 MHz, $(CD_3)_2SO$) δ 0.79−1.66 (m, 13H), 1.66−1.96 (m, 5H), 2.38−2.47 (m, 4H), 2.47−2.60 (m, 2H, overlapped with DMSO), 3.12−3.33 (m, 4H), 3.39−3.54 (m, 1H), 3.52−3.63 (m, 4H), 4.02 (t, J = 5.6 Hz, 2H), 7.21 (d, J = 5.3 Hz, 2H), 7.87 (t, J = 5.5 Hz, 1H), 8.38 (d, J = 5.6 Hz, 2H), 9.41 (bs, 1H). HRMS m/z calcd. for $C_{25}H_{42}N_7O_4S$ $[M + H]^+$, 536.3019; found, 536.2976.

*6-(2-Cyano-3-(pyridin-4-yl)guanidino)-N-(cyclohexylmethoxy)-N-(2-fluoroethyl)hexane-1-sulfonamide (**17**). N-(Cyclohexylmethoxy)-6-(1,3-dioxo-1,3-dihydro-2H-isoindol-2-yl)-1-hexanesulfonamide (**XXVIIc**).* To a solution of *O*-(cyclohexylmethyl)hydroxylamine (**VIIId**) (1.1 g, 8.51 mmol) and triethylamine (2.3 mL, 16.55 mmol) in dry dichloromethane (40 mL) at ice-bath temperature slowly for 2 h was added 6-(1,3-dioxo-1,3-dihydro-2*H*-isoindol-2-yl)hexane-1-sulfonyl chloride (**XXVb**) (3.08 g, 9.34 mmol) portion-wise. The reaction mixture was allowed gradually to warm up to room temperature (for 1 h) and evaporated. The residue was dissolved in ethyl acetate (100 mL), washed successively with water (2 × 15 mL) and brine (30 mL), and dried (Na_2SO_4). The solvent was evaporated, and the residue was dried in vacuo over P_2O_5 to afford compound **XXVIIc** (3.2 g, 89%) as crystalline solid. ^{1}H NMR (400 MHz, $CDCl_3$) δ 0.86−1.00 (m, 2H), 1.08−1.30 (m, 3H), 1.33−1.44 (m, 2H), 1.46−1.57 (m, 3H), 1.61−1.77 (m, 7H), 1.75−1.85 (m, 2H), 3.18 (m, 2H), 3.68 (t, 2H, J = 7.2 Hz), 3.80 (d, 2H, J = 6.2 Hz), 6.99 (s, 1H), 7.71 (m, 2H), 7.84 (m, 2H).

*N-(Cyclohexylmethoxy)-6-(1,3-dioxo-1,3-dihydro-2H-isoindol-2-yl)-N-(2-fluoroethyl)-1-hexanesulfonamide (**XXVIIi**).* To a solution of *N*-(cyclohexylmethoxy)-6-(1,3-dioxo-1,3-dihydro-2*H*-isoindol-2-yl)-1-hexanesulfonamide (XXVIIc) (2.11 g, 5.0 mmol), 2-fluoroethanol (0.4 g, 6.2 mmol), and triphenylphosphine (2.16 g, 8.2 mmol) in dichloromethane (40 mL) at ice-bath temperature slowly in 10 min was added a solution of diethyl azodicarboxylate (1.43 g, 8.2 mmol) in dichloromethane (1.5 mL), and the resulting mixture was stirred at this temperature for 20 min. The ice bath was removed, and then, the reaction mixture was stirred at room temperature for 3 h and evaporated. The residue was mixed with petroleum ether−ethyl acetate (4:1, 25 mL), and the obtained suspension was stirred for 30 min at ice-bath temperature and filtered. The filtrate was evaporated, and the residue was chromatographed on silica gel with toluene−ethyl acetate (9:1) as eluent to afford compound **XXVIIi** (1.57 g, 67%) as white crystals. ^{1}H NMR (400 MHz, $CDCl_3$) δ 0.90−1.06 (m, 2H), 1.09−1.33 (m, 4H), 1.33−1.45 (m, 2H), 1.45−1.79 (m, 9H), 1.83−1.95 (m, 2H), 3.07 (m, 2H), 3.54 (td, 2H, J = 5.0, 23.8 Hz), 3.68 (t, 2H, J = 7.1 Hz), 3.86 (d, 2H, J = 6.4), 4.62 (td, 2H, J = 5.0, 47.1 Hz), 7.71 (m, 2H), 7.83 (m, 2H).

*6-Amino-N-(cyclohexylmethoxy)-N-(2-fluoroethyl)-1-hexanesulfonamide (**Vi**).* *N*-(Cyclohexylmethoxy)-6-(1,3-dioxo-1,3-dihydro-2*H*-isoindol-2-yl)-*N*-(2-fluoroethyl)-1-hexanesulfonamide (**XXVIIi**) (1.53 g, 3.26 mmol) was dissolved in a mixture of ethanol (20 mL) and chloroform (10 mL), and hydrazine hydrate (0.5 mL, 103 mmol) was added. The reaction mixture was stirred at 60 °C for 2 h, left overnight at room temperature, and cooled in the refrigerator (5 °C). The precipitated solid was filtered off, and the filtrate was evaporated. The residue was chromatographed on silica gel with chloroform−methanol−30% ammonium hydroxide aqueous solution (5:1:0.15) as eluent to give compound **Vi** (0.93 g, 84%) as white crystals. ^{1}H NMR (400 MHz, $CDCl_3$) δ 0.90−1.04 (m, 2H), 1.09−1.30 (m, 3H), 1.33−1.54 (m, 6H), 1.54−1.78 (m, 6H), 1.82−2.02 (m, 4H), 2.72 (t, 2H, J = 6.9 Hz), 3.08 (m, 2H), 3.54 (td, 2H, J = 5.0, 23.6 Hz), 3.87 (d, 2H, J = 6.5), 4.62 (td, 2H, J = 5.0, 47.0 Hz).

*6-(2-Cyano-3-(pyridin-4-yl)guanidino)-N-(cyclohexylmethoxy)-N-(2-fluoroethyl)hexane-1-sulfonamide (**17**).* A mixture of 6-amino-*N*-(cyclohexylmethoxy)-*N*-(2-fluoroethyl)-1-hexanesulfonamide (**Vi**) (1.95 g, 5.76 mmol), 4-[(cyanoimino)(methylsulfanyl)methyl]-aminopyridine (**IIIa**) (1.1 g, 5.76 mmol), triethylamine (0.93 mL, 6.68 mmol), and 4-dimethylaminopyridine (0.15 g, 1.22 mmol) in dry pyridine (20 mL) was stirred at 85 °C for 20 h. The solvent was evaporated to dryness; the residue was azeotropically dried with toluene (2 × 5 mL) and then vigorously stirred with ether (30 mL) until the precipitation occurred (~2 h). The obtained suspension was filtered, and the solid material (2.7 g) was chromatographed on silica gel with chloroform−methanol−30% ammonium hydroxide aqueous solution (6:1:0.015) as eluent to give compound **17** (2.48 g, 89%) as white crystals. mp 100−102 °C. ^{1}H NMR (400 MHz, $CDCl_3$) δ 0.90−1.04 (m, 2H), 1.11−1.29 (m, 3H), 1.41 (qui, 2H, J = 7.3 Hz), 1.48−1.75 (m, 10H), 1.91 (qui, 2H, J = 7.6 Hz), 3.09 (t, 2H, J = 7.5 Hz), 3.36 (q, 2H, J = 6.6 Hz), 3.52 (dt, 2H, J = 4.9, 24.0 Hz), 3.86 (d, 2H, J = 6.5 Hz), 4.61 (dt, 2H, J = 4.9, 47.0 Hz), 5.51 (bs, 1H), 7.20 (d, 2H, J = 4.9 Hz), 7.68 (bs, 1H), 8.55 (d, 2H, J = 4.9 Hz). Anal. calcd. for $C_{22}H_{35}FN_6O_3S$: C, 54.75; H, 7.31; N, 17.41. Found: C, 54.85; H, 7.42; N, 17.50. HRMS m/z calcd. for $C_{22}H_{36}FN_6O_3S$ $[M + H]^+$, 483.2554; found, 483.2526.

Cell Culture. Human breast carcinoma MCF-7 and ovarian carcinoma A2780 were grown according to American Type Culture Collection guidelines. Cell culture media were from Invitrogen unless otherwise stated. MCF-7 was maintained in DMEM and A2780 in RPMI 1640 with GlutaMax. Media was supplemented with 10%(v/v) FCS (Perbio, Thermo Fischer Scientific), penicillin (100 U/mL), and streptomycin (0.1 mg/mL), and cells were incubated at 37 °C in an atmosphere containing 5% CO_2.

WST-1 Proliferation Assay. Cells were seeded in 96-well plates (3 × 10^3 cells/well) in culture medium (100 μL). The following day compounds were serially diluted in culture medium, and 100 μL of each dilution were added per well in triplicate to the cell culture plates. Plates were incubated (72 h, 37 °C, 5% CO_2 atmosphere), and the number of viable cells were assessed using cell proliferation reagent WST-1 (Roche, Mannheim, Germany). Reagent (10 μL) was added to each well, and after a 1 h incubation period, absorbance was measured at 450 nm subtracting absorbance at 690 nm as a reference. Data were analyzed using GraphPad Prism (GraphPad Software, CA, USA) and Calcusyn (Biosoft, Cambridge, UK) as appropriate.

Clonogenic Assays. HCT-116/APO866 resistant cell line was obtained as described previously.[42]

In vitro colony forming assays were performed essentially as previously published.[49] Briefly, HCT116 cells were cultured with compounds for the indicated times and seeded onto 35 mm dishes in agar (3% w/v) containing a sheep erythrocyte feeder layer. Agar plates were cultured for 14−21 days at 37 °C, and colonies were counted using a digital colony counter and Sorcerer image analysis software (Perceptive Instruments Ltd., SuVolk, UK). Data were analyzed using GraphPad Prism and Calcusyn as appropriate.

NAMPT Enzyme Assay. NAMPT enzyme activity was measured as described previously with minor modifications.[50,51] In this procedure, the NAMPT-catalyzed formation of ^{14}C-nicotinamide mononucleotide (NMN) was determined, using ^{14}C-nicotinamide and 5-phosphoribosyl-1-pyrophosphate (PRPP) as substrates.

For preparation of lysates, confluent HepG2 cells were washed twice with phosphate-buffered saline (PBS) (4 °C, Ca^{2+}, Mg^{2+} free), once with $NaHPO_4$ buffer, (0.01 N, pH 7.4), and scraped in $NaHPO_4$ buffer. After centrifugation (10 min, 500g, 4 °C), the pelleted cells were resuspended by pipetting in $NaHPO_4$ buffer to a concentration of approximately 10^7 cells/100 μL for HepG2 and aliquoted (200 μL aliquots in 2 mL tubes). Cells were then broken up by sonography on ice (Bandelin Sonopuls, 3 × 10 s, approximately 30% power). Cell debris was removed by centrifugation (23 000g, 90 min, 0 °C). Protamine sulfate solution (1% in $NaHPO_4$ buffer) was added to the supernatant (70 μL/mL supernatant) to precipitate DNA by

dx.doi.org/10.1021/jm4009949 | J. Med. Chem. XXXX, XXX, XXX−XXX

incubation on ice for 15 min. After centrifugation (23 000*g*, 30 min, 0 °C), aliquots of the supernatant were stored at −80 °C.

Various concentrations of inhibitor or adequate concentrations of DMSO as solvent control and cell lysates (10 μL) were added to a total of 50 μL of reaction mixture (50 mmol/L Tris−HCl pH 7.4; 2 mmol/L ATP; 5 mmol/L $MgCl_2$; 0.5 mmol/L PRPP; 6.2 μmol/L ^{14}C-nicotinamide; American Radiolabeled Chemicals, St. Louis; MO, USA) and incubated (37 °C, 1 h). The reaction was terminated by transfer into tubes containing acetone (2 mL). The whole mixture was then pipetted onto acetone-presoaked glass microfiber filters (GF/A Ø 24 mm; Whatman, Maidstone, UK). After rinsing with acetone (2 × 1 mL), filters were dried and transferred into vials with scintillation cocktail (6 mL, Betaplate Scint, PerkinElmer, Waltham, MA, USA), and radioactivity of ^{14}C-NMN was quantified in a liquid scintillation counter (Wallac 1409 DSA, Perkin−Elmer). After subtraction of blank values, NAMPT activity was normalized to total protein as measured by BCA assay (Pierce).

Xenograft Studies. The antitumor effect in vivo was tested in an A2780 (ovarian cancer) subcutaneous (sc) xenograft model in nude mice (female, NMRI/nude, Harlan or Taconic). Cancer cells were grown in RPMI with 10% FBS, washed once with PBS, and suspended in 100 μL of PBS and 100 μL of matrigel (BD) and injected sc. Treatment started at tumor volumes around 100 mm^3 (small tumors) or 500 mm^3 (large tumor). The compounds were formulated in 2% DMSO, 20% HP-β-CD, and isotonic saline at 10 mL/kg ip injection. Tumor diameters were measured during tumor growth and tumor volumes (Tv) estimated according to the following formula: Tv = (width^2 × length)/2. Mice were observed for tumor regression after 1 week or else sacrificed. The experiments were conducted at Topotarget A/S, Copenhagen and approved by the Experimental Animal Inspectorate, Danish Ministry of Justice.

Pharmacokinetic Analysis. Mouse plasma samples were prepared for analysis by protein precipitation on Sirocco plates (Waters, Milford, MA, USA). A Waters Acquity UPLC system with a Quattro Premier MS-MS system was used for separation and detection. Acetonitrile containing 1 μg/mL internal standard was used in the ratio 3:1 (v/v) for precipitation. Separation was performed with an acetonitrile/0.05% formic acid gradient on a Acquity UPLC BEH C18, 2.1 mm × 50 mm, 1.7 μm reversed-phase column (Waters A/S) operated at 40 °C. Detection was performed using electrospray MRM in the positive mode. Pharmacokinetic parameters were calculated using noncompartmental analysis methods as included in WinNonlin ver 5.02 (Pharsight, CA, USA).

Docking Analysis. The structure was downloaded from the protein data bank (PDB ID 2GVJ) and prepared for docking using the built-in protein preparation wizard in Maestro version 9.3. During this process, bond orders were assigned, and hydrogens were added to the crystal structure. Furthermore, the four seleno-methionines that had been incorporated to allow for better X-ray diffraction were changed to cysteines (chain A: residues 368 and 372; chain B: residues 368 and 372). The docking was carried out using Glide version 5.8 in extra precision (XP) mode. The ligands were docked flexibly, and nitrogen inversions and ring flips were allowed. The van der Waals radii of the nonpolar ligand atoms (partial charge < 0.15) were scaled by a factor of 0.8 to accommodate slightly inaccurate initial dockings. A postdocking minimization was carried out for the best 25 poses for each ligand, and finally, the 10 best poses were reported.

DFT Analysis. This study was carried out using Jaguar version 8.0.[52] DFT used the B3LYP functional[53−55] with added d3 corrections[56,57] to account for dispersion interactions. We used the 6-31G** basis set[58] throughout.

■ ASSOCIATED CONTENT

Supporting Information

Experimental procedures; analytical and spectral data for all intermediate and final compounds; computation chemistry docking scores and associated docking poses. This material is available free of charge via the Internet at http://pubs.acs.org.

■ AUTHOR INFORMATION

Corresponding Author

*Phone: +45 35 33 62 31; fax: +45 35 33 60 41; e-mail: fb@sund.ku.dk.

Present Addresses

▽Mette K. Christensen: Novo Nordisk A/S, 2880 Bagsværd, Denmark.

○Annemette Thougaard: H. Lundbeck A/S, 2500 Valby, Denmark.

◆Søren Jensby Nielsen: Nuevolotion A/S 2100 Copenhagen, Denmark.

¶Peter B. Jensen: Medical Prognosis Institute, 2970 Hørsholm, Denmark.

▲Kamille D. Erichsen: BioAdvice A/S, 2950 Vedbæk, Denmark.

Notes

The authors declare the following competing financial interest(s): Author J.T. is an employee of Topotarget A/S. Authors K.D.E, M.K.C., U.H.O., A.T., S.J.N., M.S., P.B.J., and F.B. are previous employees of Topotarget A/S.

■ ACKNOWLEDGMENTS

We thank Anja Barnikol-Oettler for expert technical assistance with the NAMPT enzymatic assay and support from the German Research Council (DFG, KFO152-TP7) and the Leipzig LIFE (LIFE Child Health and Child Obesity) program to W.K. P.F. was supported by a Sapare Aude grant from the Danish Council for Independent Research no. 11-105487. We thank Nicolaj Høj and Søren Ryborg for organic synthesis assistance.

■ ABBREVIATIONS USED

cADPR, cyclic ADP ribose; NAADP, nicotinic acid adenine dinucleotide phosphate; AUC, area under the curve; bid, twice daily; DMEM, Dulbecco's modified eagle medium; HRMS, high-resolution mass spectrometry; IC_{50}, concentration of a test compound that produces half maximal inhibition; LC-MS, liquid chromatography−mass spectrometry; MTD, maximum tolerated dose; t_{max}, time of maximum drug concentration; C_{max}, maximum drug concentration; V_z, volume of distribution; CL, drug clearance; NMR, nuclear magnetic resonance; SAR, structure−activity relationship; SD, standard deviation

■ REFERENCES

(1) Khan, J. A.; Forouhar, F.; Tao, X.; Tong, L. Nicotinamide adenine dinucleotide metabolism as an attractive target for drug discovery. *Expert Opin. Ther. Targets* **2007**, *11* (5), 695−705.

(2) Diefenbach, J.; Burkle, A. Introduction to poly(ADP-ribose) metabolism. *Cell. Mol. Life Sci.* **2005**, *62* (7−8), 721−730.

(3) Ziegler, M. New functions of a long-known molecule. Emerging roles of NAD in cellular signaling. *Eur. J. Biochem.* **2000**, *267* (6), 1550−1564.

(4) Saunders, L. R.; Verdin, E. Sirtuins: critical regulators at the crossroads between cancer and aging. *Oncogene* **2007**, *26* (37), 5489−5504.

(5) Genazzani, A. A.; Billington, R. A. NAADP: An atypical Ca^{2+}-release messenger. *Trends Pharmacol. Sci.* **2002**, *23*, 165−167.

(6) Malavasi, F.; Deaglio, S.; Funaro, A.; Ferrero, E.; Horenstein, A. L.; Ortolan, E.; Vaisitti, T.; Aydin, S. Evolution and function of the ADP ribosyl cyclase/CD38 gene family in physiology and pathology. *Physiol. Rev.* **2008**, *88*, 841−886.

(7) Hageman, G. J.; Stierum, R. H. Niacin, poly(ADP-ribose) polymerase-1 and genomic stability. *Mutat. Res.* **2001**, *475* (1−2), 45−56.

(8) Lengauer, C.; Kinzler, K. W.; Vogelstein, B. Genetic instabilities in human cancers. *Nature* **1998**, *396* (6712), 643−649.
(9) Nomura, F.; Yaguchi, M.; Togawa, A.; Miyazaki, M.; Isobe, K.; Miyake, M.; Noda, M.; Nakai, T. Enhancement of poly-adenosine diphosphate-ribosylation in human hepatocellular carcinoma. *J. Gastroenterol. Hepatol.* **2000**, *15* (5), 529−535.
(10) Hufton, S. E.; Moerkerk, P. T.; Brandwijk, R.; de Bruïne, A. P.; Arends, J.-W.; Hoogenboom, H. R. A profile of differentially expressed genes in primary colorectal cancer using suppression substractive hybridization. *FEBS Lett.* **1999**, *463*, 77−82.
(11) van Beijnum, J. R.; Moerker, P. T.; Gerbers, A. J.; de Bruïne, A. P.; Arends, J.-W.; Hoogenboom, H. R.; Hufton, S. E. Target validation for genomics using peptide-specific phage antibodies: a study of five gene products overexpressed in colorectal cancer. *Int. J. Cancer* **2002**, *101*, 118−127.
(12) Foster, J. W.; Moat, A. G. Nicotinamide adenine dinucleotide biosynthesis and pyridine nucleotide cycle metabolism in microbial systems. *Microbiol. Rev.* **1980**, *44* (1), 83−105.
(13) Magni, G.; Amici, A.; Emanuelli, M.; Orsomando, B.; Raffaelli, N.; Ruggieri, S. Enzymology of NAD+ homeostasis in man. *Cell. Mol. Life Sci.* **2004**, *61* (1), 19−34.
(14) Preiss, J.; Handler, P. Enzymatic synthesis of nicotinamide mononucleotide. *J. Biol. Chem.* **1957**, *225*, 759−770.
(15) Preiss, J.; Handler, P. Biosynthesis of diphosphopyridine nucleotide. I. Identification of intermediates. *J. Biol. Chem.* **1958**, *233*, 488−492.
(16) Rongvaux, A.; Andris, F.; van Gool, F.; Leo, O. Reconstructing eukaryotic NAD metabolism. *Bioessays* **2003**, *25*, 683−690.
(17) Gross, J. W.; Rajavel, M.; Grubmeyer, C. Kinetic mechanism of nicotinic acid phosphoribosyltransferase: Implications for energy coupling. *Biochemistry* **1998**, *37*, 4189−4199.
(18) Olesen, U. H.; Hastrup, N.; Sehested, M. Expression patterns of nicotinamide phosphoribosyltransferase and nicotinic acid phosphoribosyltransferase in human malignant lymphomas. *APMIS.* **2011**, *119* (4−5), 296−303.
(19) Shackelford, R. E.; Bui, M. M.; Coppola, D.; Hakam, A. Overexpression of nicotinamide phosphoribosyltransferase in ovarian cancers. *Int. J. Clin. Exp. Pathol.* **2010**, *3* (5), 522−527.
(20) Wang, B.; Hasan, M. K.; Alvarado, E.; Huan, H.; Wu, H.; Chen, W. Y. NAMPT overexpression in prostate cancer and its contribution to tumor cell survival and stress response. *Oncogene* **2011**, *30* (8), 907−21.
(21) Hasmann, M.; Schemainda, I. FK866, a highly specific noncompetitive inhibitor of nicotinamide phosphoribosyltransferase, represents a novel mechanism for induction of tumor cell apoptosis. *Cancer Res.* **2003**, *63*, 7436−7442.
(22) Schou, C.; Ottosen, E. R.; Petersen, H. J.; Björkling, F.; Latini, S.; Hjarnaa, P. V.; Bramm, E.; Binderup, L. Novel cyanoguanidines with potent oral antitumour activity. *Bioorg. Med. Chem. Lett.* **1997**, *7* (24), 3095−3100.
(23) Colombano, G.; Travelli, T.; Galli, U.; Caldarelli, A.; Chini, M. G.; Canonico, P. L.; Sorba, G.; Bifulco, G.; Tron, G. C.; Genazzani, A. A. A novel potent nicotinamide phosphoribosyltransferase inhibitor synthesized via click chemistry. *J. Med. Chem.* **2010**, *53*, 616−623.
(24) Fleischer, T. C.; Murphy, B. R.; Flick, J. S.; Terry-Lorenzo, R. T.; Gao, Z.-H.; Davis, T.; McKinnon, R.; Ostanin, K.; Willardsen, J. A.; Boniface, J. J. Chemical proteomics identifies Nampt as the target of CB30865, an orphan cytotoxic compound. *Chem. Biol.* **2010**, *17*, 659−664.
(25) Carlson, R. O.; Willardsen, J. A.; Lockman, J. W.; Bradford, C. L.; Patton, J. S.; Papac, D. I.; Boniface, J. J.; Yager, K.; Baichwal, V. R. Pharmacokinetics, anti-tumor activity and therapeutic index of Nampt inhibitor MPC-8640 in mice. In *Mol. Cancer Ther.*, Proceedings of the AACR-NCI-EORTC International Conference: Molecular Targets and Cancer Therapeutics, San Francisco, CA, November 12−16, 2011; AACR: Philadelphia, PA, 2011; Vol. *10*, (11 Suppl.), Abstract nr B137.
(26) Cea, M.; Zoppoli, G.; Bruzzone, S.; Fruscione, F.; Moran, E.; Garuti, A.; Rocco, I.; Cirmena, G.; Casciaro, S.; Olcese, F.; Pierri, I.; Cagnetta, A.; Ferrando, F.; Ghio, R.; Gobbi, M.; Ballestrero, A.; Patrone, F.; Nencioni, A. APO866 activity in hematologic malignancies: A preclinical in vitro study. *Blood* **2009**, *113*, 6035−6037.
(27) Nahimana, A.; Attinger, A.; Aubry, D.; Greaney, P.; Ireson, C.; Thougaard, A. V.; Tjørnelund, J.; Dawson, K. M.; Dupuis, M.; Duchosal, M. A. The NAD biosynthesis inhibitor APO866 has potent antitumor activity against hematologic malignancies. *Blood* **2009**, *113*, 3276−3286.
(28) Galli, U.; Travelli, C.; Massarotti, A.; Fakhfouri, G.; Rahimian, R.; Tron, G. C.; Genazzani, A. A. Medicinal chemistry of nicotinamide phosphoribosyltransferase (NAMPT) Inhibitors. *J. Med. Chem.* **2013**, *56* (16), 6279−6296.
(29) Olesen, U. H.; Christensen, M. K.; Björkling, F.; Jäättelä, M.; Jensen, P. B.; Sehested, M.; Nielsen, S. J. Anticancer agent CHS-828 inhibits cellular synthesis of NAD. *Biochem. Biophys. Res. Commun.* **2008**, *367* (4), 799−804.
(30) Watson, M.; Roulston, A.; Belec, L.; Billot, X.; Marcellus, R.; Bédard, D.; Bernier, C.; Branchaud, S.; Chan, H.; Dairi, K.; Gilbert, K.; Goulet, D.; Gratton, M.-O.; Isakau, H.; Jang, A.; Khadir, A.; Koch, E.; Lavoie, M.; Lawless, M.; Nguyen, M.; Paquette, D.; Turcotte, E.; Berger, A.; Mitchell, M.; Shore, G. C.; Beauparlant, P. The small molecule GMX1778 is a potent inhibitor of NAD^+ biosynthesis: Strategy for enhanced therapy in nicotinic acid phosphoribosyltransferase 1-deficient tumors. *Mol. Cell. Biol.* **2009**, 5872−5888.
(31) Khan, J. A.; Tao, X.; Tong, L. Molecular basis for the inhibition of human NMPRTase, a novel target for anticancer agents. *Nat. Struct. Mol. Biol.* **2006**, *13*, 582−588.
(32) Holen, K.; Saltz, L. B.; Hollywood, E.; Burk, K.; Hanauske, A. R. The pharmacokinetics, toxicities, and biologic effects of FK866, a nicotinamide adenine dinucleotide biosynthesis inhibitor. *Invest. New Drugs* **2008**, *26*, 45−51.
(33) Hovstadius, P.; Larsson, R.; Jonsson, E.; Skov, T.; Kissmeyer, A. M.; Krasilniko, V. K.; Bergh, J.; Karlsson, M. O.; Lonnebo, A.; Ahlgren, J. A phase I study of CHS 828 in patients with solid tumour malignancy. *Clin. Cancer Res.* **2002**, *8*, 2843−2850.
(34) Pishvaian, M.; Marshall, J.; Hwang, J.; Malik, S.; He, A.; Deeken, J.; Kelso, C.; Cotaria, I.; Berger, M. A. Phase I trial of GMX1777, an inhibitor of nicotinamide phosphoribosyl transferase (NAMPRT), given as a 24-h infusion. In *J. Clin. Oncol.*, ASCO Annual Meeting Proceedings (Post-Meeting Edition), Orlando, FL, May 29 to June 2, 2009, ASCO: Alexandria, VA, 2009; Vol. *26*, No 15S (May 20 Supplement).
(35) Binderup, E.; Björkling, F.; Hjarnaa, P. V.; Latini, S.; Baltzer, B.; Carlsen, M.; Binderup, L. EB1627: A soluble prodrug of the potent anticancer cyanoguanidine CHS828. *Bioorg. Med. Chem. Lett.* **2005**, *15*, 2491−2494.
(36) Beauparlant, P.; Bédard, D.; Bernier, C.; Chan, H.; Gilbert, K.; Goulet, D.; Gratton, M.-O.; Lavoie, M.; Roulston, A.; Turcotte, E.; Watson, M. Preclinical development of the nicotinamide phosphoribosyl transferase inhibitor prodrug GMX1777. *Anti-Cancer Drugs* **2009**, *20*, 346−354.
(37) Skelton, L. A.; Ormerod, M. G.; Titley, J.; Kimbell, R.; Brunton, L. A.; Jackman, A. L. A novel class of lipophilic quinazoline-based folic acid analogues: Cytotoxic agents with a folate-independent locus. *Br. J. Cancer* **1999**, *79* (11/12), 1692−1701.
(38) Orwig, K. S.; Dix, T. A. Synthesis of C^{α} methylated carboxylic acids: isosteres of arginine and lysine for use as N-terminal capping residues in polypeptides. *Tetrahedron Lett.* **2005**, *46* (41), 7007−7009.
(39) Butera, J. A.; Antane, M. M.; Antane, S. A.; Argentieri, T. M.; Freeden, C.; Graceffa, R. F.; Hirth, B. H.; Jenkins, D.; Lennox, J. R.; Matelan, E.; Norton, N. W.; Quagliato, D.; Sheldon, J. H.; Spinell, W.; Warga, D.; Wojdan, A.; Woods, M. Design and SAR of novel potassium channel openers targeted for urge urinary incontinence. 1. *N*-cyanoguanidine bioisosteres possessing in vivo bladder selectivity. *J. Med. Chem.* **2000**, *43*, 1187−1202.
(40) Humljan, J.; Gobec, S. Synthesis of *N*-phthalimido *β*-aminoethanesulfonyl chlorides: The use of thionyl chloride for a simple and efficient synthesis of new peptidosulfonamide building blocks. *Tetrahedron Lett.* **2005**, *43*, 4069−4072.

(41) Kim, M. K.; Lee, J. H.; Kim, H.; Park, S. J.; Kim, S. H.; Kang, G. B.; Lee, Y. S.; Kim, J. B.; Kim, K. K.; Suh, S. W.; Eom, S. H. Crystal structure of visfatin/pre-B cell colony-enhancing factor 1/nicotinamide phosphorybosyltransferase, free and in complex with the anti-cancer agent FK-866. *J. Mol. Biol.* **2006**, *362*, 66−77.
(42) Olesen, U. H.; Petersen, J. G.; Garten, A.; Kiess, W.; Yoshino, J.; Imai, S.; Christensen, M. K.; Fristrup, P.; Thougaard, A. V.; Björkling, F.; Jensen, P. B.; Nielsen, S. J.; Sehested, M. Target enzyme mutations are the molecular basis for resistance towards pharmacological inhibition of nicotinamide phosphoribosyltransferase. *BMC Cancer.* **2010**, *10*, 677.
(43) Murthi, K. K.; Köstler, R.; Smith, C.; Brandstetter, T.; Kluge, A. F. *Derivatives of squaric acid with anti-proliferative activity*. EU Pat. Appl. EP 1 674 457 A1, 2004.
(44) Linderoth, L.; Fristrup, P.; Hansen, M.; Melander, F.; Madsen, R.; Andresen, T. L.; Peters, G. H. Mechanistic study of the $sPLA_2$-mediated hydrolysis of a thio-ester pro anticancer ether lipid. *J. Am. Chem. Soc.* **2009**, *131*, 12193−12200.
(45) Kornet, M. J. Potential antifibrillatory agents. *N*-(ω-amino-alkoxy) phthalimides. *J. Med. Chem.* **1966**, *9*, 269.
(46) Deraeve, C.; Bon, R. S.; Stigter, E. A.; Wetzel, S.; Waldmann, H.; Guo, Z.; Blankenfeldt, W.; Alexandrov, K.; Goody, R. S.; Wu, Y. W.; DiLucrezia, R.; Wolf, A.; Menninger, S.; Choidas, A. Psoromic acid is a selective and covalent rab-prenylation inhibitor targeting autoinhibited RabGGTase. *J. Am. Chem. Soc.* **2012**, *134*, 7384−7391.
(47) Boehringer Ingelheim International, GMBH, Patent: WO2009/112565 A1, 2009.
(48) Zhao, X.; Jiang, X. K.; Shi, M.; Yu, Y. H.; Xia, W.; Li, Z. T. Self-assembly of novel [3]- and [2]-rotaxanes with two different ring components: Donor−acceptor and hydrogen bonding interactions and molecular-shuttling behavior. *J. Org. Chem.* **2001**, *66* (21), 7035−7043.
(49) Natarajan, A.; Fan, Y.-H.; Chen, H.; Guo, Y.; Iyasere, J.; Harbinski, F.; Christ, W. J.; Aktas, H.; Halperin, J. A. 3,3-Diaryl-1,3-dihydroindol-2-ones as antiproliferatives mediated by translation initiation inhibition. *J. Med. Chem.* **2004**, *47*, 1882−1885.
(50) Elliott, G. C.; Ajioka, J.; Okada, C. Y. A rapid procedure for assaying nicotinamide phosphoribosyl-transferase. *Anal. Biochem.* **1980**, *107*, 199−205.
(51) Garten, A.; Petzold, S.; Barnikol-Oettler, A.; Körner, A.; Thasler, W. E.; Kratzsch, J.; Kiess, W.; Gebhardt, R. Nicotinamide phosphoribosyltransferase (NAMPT/PBEF/visfatin) is constitutively released from human hepatocytes. *Biochem. Biophys. Res. Commun.* **2010**, *391*, 376−381.
(52) *Jaguar*, version 8.0 release 47; Schrodinger, LLC: New York, 2013.
(53) Becke, A. D. Density-functional thermochemistry. III. The role of exact exchange. *J. Chem. Phys.* **1993**, *98*, 5648−5652.
(54) Becke, A. D. A new mixing of Hartree−Fock and local density-functional theories. *J. Chem. Phys.* **1993**, *98*, 1372−1377.
(55) Lee, C.; Yang, W.; Parr, R. G. Development of the Colle-Salvetti correlation-energy formula into a functional of the electron density. *Phys. Rev. B* **1988**, *37*, 785−789.
(56) Elstner, M.; Hobza, P.; Frauenheim, T.; Suhai, S.; Kaxiras, E. Hydrogen bonding and stacking interactions of nucleic acid base pairs: A density-functional-theory based treatment. *J. Chem. Phys.* **2001**, *114*, 5149−5155.
(57) Grimme, S. Accurate description of van der Waals complexes by density functional theory including empirical corrections. *J. Comput. Chem.* **2004**, *25*, 1463−1473.
(58) Ditchfield, R.; Hehre, W. J.; Pople, J. A. Self-consistent molecular-orbital methods. IX. An extended Gaussian-type basis for molecular-orbital studies of organic molecules. *J. Chem. Phys.* **1971**, *54*, 724−728.